



A review of the Iberian Sphingonotini with description of two novel species (Orthoptera: Acrididae: Oedipodinae)

MARTIN HUSEMANN¹, DAVID LLUCIÀ-POMARES² and AXEL HOCHKIRCH^{3*}

¹Biology Department, Baylor University, Waco, TX 76798, USA

²Sant Jaume, 8, casa 1; 08184, Palau-Solità i Plegamans (Barcelona), Spain

³Department of Biogeography, Trier University, D-54286 Trier, Germany

Received 28 June 2012; revised 21 January 2013; accepted for publication 29 January 2013

The genus *Sphingonotus* Fieber, 1853 is one of the most species-rich grasshopper genera in the world. We studied the morphology of *c.* 1000 individuals from the Iberian Peninsula to review the taxonomy of the genus and its relatives. Moreover, we inferred a molecular phylogeny of the Iberian Sphingonotini based on two mitochondrial genes. The Iberian and north-west African Sphingonotini comprise two recent radiations, within which the genetic relationships are not fully resolved. A multivariate morphometric analysis showed that *S. azurescens* (Rambur, 1838) and *S. morini* (Defaut, 2005) can be clearly discriminated, supporting their species status. Based upon the combined data, the genus *Granada* Koçak & Kemal, 2008 is synonymized with *Sphingonotus* Fieber, 1853 and its type species re-assigned to *Sphingonotus imitans* Brunner von Wattenwyl, 1882 **comb. rev.** The data also supported species rank for *Sphingonotus lusitanicus* Ebner, 1941 **comb. rev.** *Oedipoda callosa* Fieber, 1853 is considered as *nomen dubium*. Two novel species are described: *Sphingonotus (Neosphingonotus) almeriense* Lluçia-Pomares **sp. nov.** and *Sphingonotus (Neosphingonotus) nodulosus* Lluçia-Pomares **sp. nov.** from the southern part of the Iberian Peninsula. The new species are compared with other Iberian Sphingonotini and a key to the species is provided.

© 2013 The Linnean Society of London, *Zoological Journal of the Linnean Society*, 2013, 168, 29–60.
doi: 10.1111/zoj.12023

ADDITIONAL KEYWORDS: biodiversity – Iberian Peninsula – Mediterranean – mtDNA – *Sphingonotus* – stridulatory apparatus – taxonomy.

INTRODUCTION

Mapping species richness and clarifying the status of animal and plant taxa is an important task in the face of recent biodiversity decline (Kim & Byrne, 2006). In this context, biodiversity hotspots deserve special attention as they play a crucial role for nature conservation (Brooks *et al.*, 2002). The Mediterranean is considered an important biodiversity hotspot (Medail & Quezel, 1999; Brooks *et al.*, 2006). The main reason for its great species richness and endemism is believed to be the climatic stability of this region compared with

temperate regions (Hewitt, 2000). It is widely accepted that the Mediterranean served as a refuge during past climatic oscillations. The majority of European thermophilous species retreated into five main refugia during the Pleistocene: the Iberian Peninsula, the Apennine Peninsula, the Balkans, Anatolia, and North Africa (Hewitt, 1999). The isolation of these refugia during glacial periods resulted in allopatric speciation events and in the accumulation of biodiversity in the Mediterranean (Cowling *et al.*, 1996). However, it is also evident that multiple smaller refugia occurred within these main refugial regions (Gómez & Lunt, 2006).

While in pure morphological studies cryptic species might be overlooked, molecular genetic markers

*Corresponding author. E-mail: hochkirch@uni-trier.de

provide a modern toolbox for studying taxonomic, systematic, and evolutionary questions and offer opportunities for detecting cryptic biodiversity (Wilcox *et al.*, 1997; Hebert *et al.*, 2004; Hochkirch & Husemann, 2008). During recent decades the application of molecular tools has uncovered many species that have formerly been undetected due to inconspicuous morphology (Kiefer *et al.*, 2002; Smith *et al.*, 2006; Hochkirch & Husemann, 2008; Hochkirch & Görzig, 2009; Vieites *et al.*, 2009). Taxa with similar ecological niches often share similar morphologies as a result of convergence (Husemann *et al.*, 2012) and therefore are ideal candidates for discovering novel species. The grasshopper genus *Sphingonotus* Fieber, 1852 represents a good example of such a taxon. It currently contains 142 described species, 39 of which occur in the Mediterranean (Eades *et al.*, 2013). The genus comprises three subgenera, with 127 species in the subgenus *Sphingonotus* Fieber, 1852, 12 species in the subgenus *Neosphingonotus* Benediktov, 1998, and three in the subgenus *Parasphingonotus* Benediktov & Husemann, 2009. Morphologically, these three subgenera are distinguished by their stridulatory mechanisms. The subgenus *Sphingonotus* possesses the typical Oedipodinae type of stridulatory mechanism (serrated intercalary vein), which is absent in other Acrididae, while the other two subgenera possess novel stridulatory mechanisms. In the subgenus *Neosphingonotus* the serration of the intercalary vein is usually lost [except for some individuals of *S. savignyi* Saussure, 1884, *S. morini* (Default, 2005), and *S. azurescens* (Rambur, 1838)], but thickened, elevated cross-veinlets between radius and media always exist. In the subgenus *Parasphingonotus* the radius is serrated instead of the intercalary vein (Husemann, Ray & Hochkirch, 2011). Many *Sphingonotus* species are morphologically rather difficult to distinguish (Hochkirch & Husemann, 2008). Thus, the genus *Sphingonotus* represents an interesting target for phylogenetic and taxonomic studies.

We studied the morphology of members of the genus *Sphingonotus* from the Iberian Peninsula and some species from northern Africa and inferred a phylogeny based upon sequences of two mitochondrial genes (12S rRNA, NADH-dehydrogenase subunit 5) to unravel the systematic relationships of the Iberian *Sphingonotini*. In course of this study, we detected two hitherto undescribed morphologically and genetically well-defined species from the southern parts of the Iberian Peninsula, which we subsequently describe. As several new species of *Sphingonotus* have been described from the Iberian peninsula in recent years (e.g. Default, 2005c; Lluçà-Pomares, 2006), we also provide a key to the Iberian species and perform additional taxonomic changes, but only if the molecu-

lar phylogeny is in line with morphological traits. Furthermore, we used multivariate morphometrics to distinguish two closely related species: *S. azurescens* and *S. morini*.

MATERIAL AND METHODS

PHYLOGENETIC ANALYSIS

Seventy-eight specimens of European and north-west African Sphingonotini species were obtained between 2002 and 2012 (see Supporting Information, Table S1). Specimens were stored either in a freezer or in 99% ethanol p.a. We chose two North African Oedipodinae species, *Helioscirtus capsitanus* (Bonnet, 1884) and *Sphingoderus carinatus* (Saussure, 1888), as outgroups. DNA was extracted from thoracic or femoral muscle tissue using the DNeasy Blood and Tissue Kit (Qiagen, Hilden, Germany) following the manufacturer's protocol. Two mitochondrial gene fragments (ND5: 1059 bp, 12S rRNA: 350 bp) were amplified and sequenced using slightly modified primers based upon Hochkirch (2001). We used the HotMasterMix (Eppendorf, Hamburg, Germany) and the HotStarTaq Master Mix Kit (Qiagen) for amplification. The PCR product was purified using the Qiaex II Gel Extraction Kit (Qiagen) or the Roche PCR product purification kit (Roche, Risch, Switzerland) following the manufacturers' protocols. Sequencing was performed with the Big Dye sequencing kit (Perkin Elmer, Altrincham, UK) for sequencing reactions run on a Perkin-Elmer ABI automated sequencer or with the DYEnamic ET Terminator Cycle Sequencing Premixkit (GE Healthcare, Munich, Germany) for runs on a MEGAbase 1000 automated sequencer (GE Healthcare). Previously published sequences (Hochkirch & Husemann, 2008, GenBank accession nos. EU266710–266746) were also included in the analysis. All DNA sequences were corrected and aligned by eye; ambiguous ends of the fragments were trimmed. Sequences were deposited in GenBank (accession numbers in Table S1). We first used MrModeltest 2.2 (Nylander, 2004) to determine the best-fitting substitution model for each gene separately. The best-fitting substitution model chosen through the Akaike information criterion (AIC) was GTR+I+G for both genes. To examine whether the data set could be concatenated, a partition-homogeneity test (Farris *et al.*, 1995) was run in PAUP 4.0b10* (Swofford, 2002) and significance was estimated with 1000 repartitions. This test did not indicate any conflicting phylogenetic signals between the data sets ($P = 0.80$). Therefore, we analysed the concatenated data set (1400 bp) in MrBayes 3.1.1 (Ronquist & Huelsenbeck, 2003). We ran the Monte Carlo Markov chain for three million generations,

sampling every 1000 generations. The first 1000 trees were discarded as burn-in, after checking for stationary and convergence of the chains in tracer 1.5 (Rambaut & Drummond, 2009). Posterior probabilities are given as statistical branch support.

MORPHOLOGICAL ANALYSIS

Three males and six females from the Parque Natural Cabo de Gata-Níjar, Almería, Spain (*S. almeriense* sp. nov.) and 18 males and six females from the southern part of the Iberian Peninsula (*S. nodulosus* sp. nov.) were studied in detail and compared with Iberian, northern African, Canarian, and some other European species of *Sphingonotus*. We dissected and hand drew the genitalia of a male of each species according to the method described by Hochkirch (2001). Moreover, we dissected the forewings of specimens of *S. finotianus* (Saussure, 1886), *S. tricinctus* (Walker, 1870) from Tunisia, *S. rubescens* (Walker, 1870) from La Gomera, *S. almeriense* sp. nov. from Spain (described below), as well as a specimen from Morocco, which is morphologically close to *S. morini*. The stridulatory apparatus was examined and photographed by scanning electron microscopy using a Zeiss DSM 962 at the University of Osnabrück and an LEO 1455 VP at the Natural History Museum (London). For the Zeiss DSM 962 wings were air dried and then coated with a thin gold layer. The LEO 1455 VP uses variable pressure and specimens can be introduced into the sample chamber of the microscope without prior preparation and coating.

The general morphometric analyses were based on the study of 486 males and 470 females of Iberian Sphingonotini; the studied characters are shown in Table 1. The measurements were taken with an ocular micrometer in a microscope (Olympus SZ-4045-F with a 110AL2× lens). All biometric values are given in millimetres. Most material has been deposited in the collection of David Lluçà-Pomares (Palau-Solità i Plegamans, Barcelona, Spain). Otherwise, the depository is mentioned. Abbreviations of depositories are as follows: ANSP, Academy of Natural Sciences, Philadelphia, USA; DBTU, Department of Biogeography of Trier University, Trier, Germany; MCNB, Museu de Ciències Naturals de Barcelona, Barcelona, Spain; NHM, Natural History Museum, London, UK; MNCN, Museo Nacional de Ciencias Naturales, Madrid, Spain; MNHN, Muséum National d'Histoire Naturelle, Paris, France; JIY, Jorge Íñiguez Yarza private collection, Olías del Rey, Toledo, Spain.

Many of the characters that have been commonly used in the differential diagnoses of former studies (e.g. Mistshenko, 1936; Harz, 1975) are intraspecifically highly variable and therefore not useful for

identification: for example, colours of the hind tibiae and inner part of the post femora, shape of the lower hind angle of the paranota, shape of the fastigial foveolae, shape of the mesosternal interspace, situation of the pronotal sulcus, and rugosity of the pronotum and of the female ovipositor valves. Other characters have meanwhile been shown to be of higher taxonomic value, particularly the outer and inner genitalia (cerci, male supra-anal plate, female ovipositor, subgenital plate, epiphallus; Husemann *et al.*, 2011). The nomenclature of the male supra-anal plate is illustrated in Fig. 8A. The maximum width of the tegmen is either found at the precostal lobe (WTl) or at the apex of the media (WTm) and can only be measured in fixed specimens with fully spread wings. As the serration of the intercalary vein correlates with tegmen length, we standardized this measure by counting the number of teeth per 5% of tegmen length. We generally counted the number of teeth at the end of the precostal lobe (which usually coincides with the posterior margin of the first dark band of the tegmina), as the serration density increases posteriorly.

The discrimination of *S. azurescens* and *S. morini* is particularly difficult with the existing taxonomic literature. To test, if these two species can be clearly distinguished morphologically, we used multivariate morphometrics. We studied 27 morphometric characters of 226 specimens sampled across the Iberian Peninsula (*S. azurescens*: 36 males, 32 females; *S. morini*: 71 males, 71 females; as well as three males of unknown species identity). These specimens included material from the type localities of both species. We first used a principal component analysis (PCA) to investigate, if a reduction of dimensions already separates the groups according to species and sexes (using z-transformed data). Afterwards, a stepwise discriminant analysis was computed to maximize separation between the four groups (2 species × 2 sexes) using Wilks' Lambda (an inverse measure) as optimality criterion. The significance of each parameter was calculated by univariate F-statistics based on Wilks' Lambda (see also Hochkirch, 2001).

RESULTS

MOLECULAR PHYLOGENY

Our phylogenetic analysis revealed three major clades of *Sphingonotus* for the Iberian Peninsula and in north-west Africa (Fig. 1). These three clades are not in line with the current taxonomic subdivision into three subgenera. One clade included only one species, *Sphingonotus octofasciatus* (Serville, 1838), which branched as sister taxon to *Sphingoderus carinatus* (one of the two outgroups). Based upon its

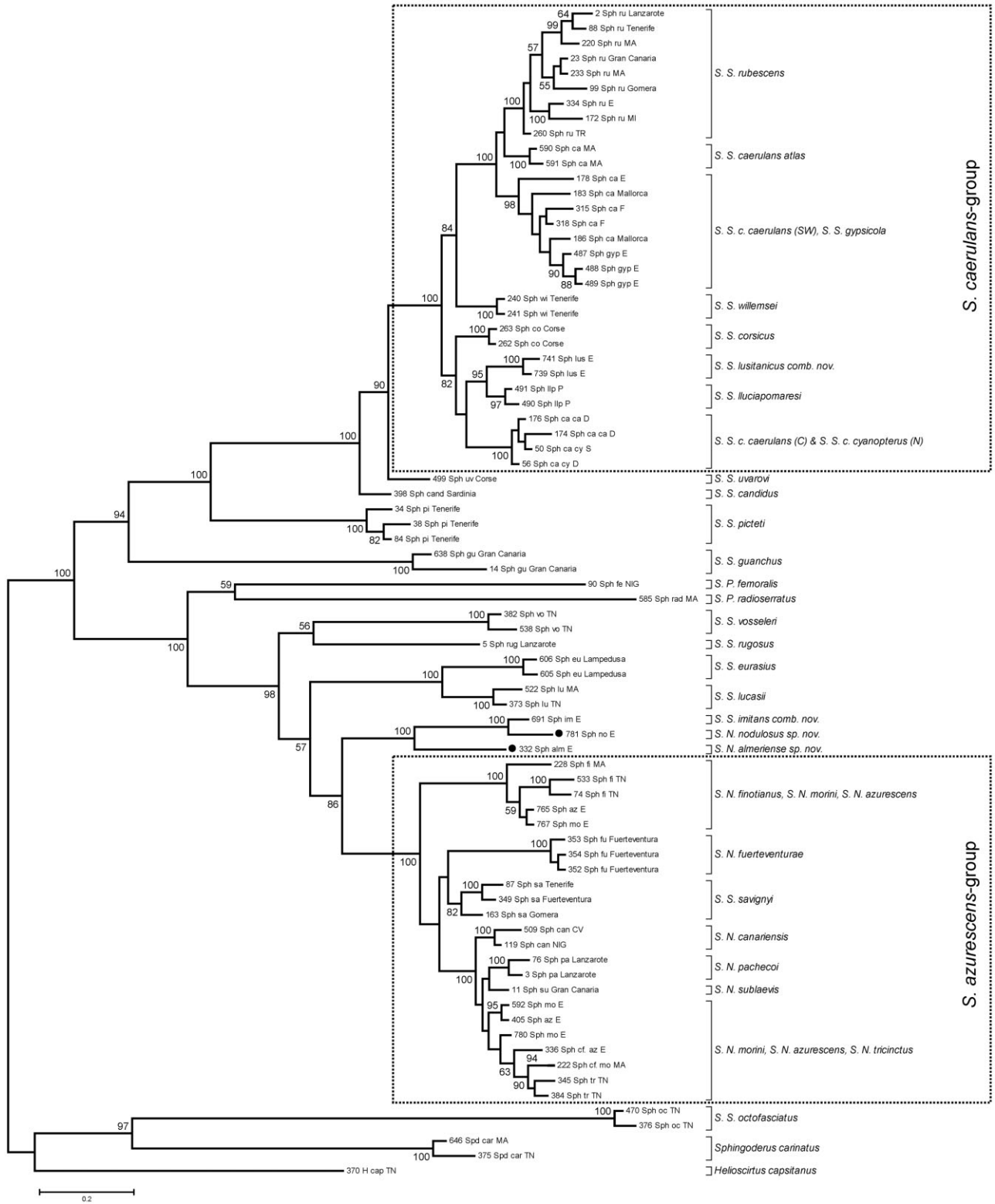


Figure 1. Bayesian consensus tree for the combined data set (NADH-dehydrogenase subunit 5 and 12S rRNA). Numbers represent percentage posterior probabilities from the Bayesian analysis. Filled circles indicate the position of the new species. Country abbreviations: E, Spain; S, Sweden; TN, Tunisia; D, Germany; MA, Morocco; NIG, Niger; TR, Turkey; F, France; I, Italy; CV, Cape Verde.

phylogenetic position it might deserve to be placed in its own genus, but this would require a more comprehensive study of other morphologically distinct *Sphingonotus* species, such as *Sphingonotus nebulosus* (Fischer von Waldheim, 1846). The other two main clades are also not in line with the current subgeneric assignments, which are based upon the unique (apomorphic) stridulatory mechanisms in two of the subgenera compared with the plesiomorphic trait (serrated intercalary vein) in the subgenus *Sphingonotus*. The subgenera *Neosphingonotus* and *Sphingonotus* are both polyphyletic, but we keep them as valid subgenera for now as they are morphologically well defined, which helps to organize this species-rich genus. A complete cladistic approach based upon genetic data alone would either require complete synonymization of all subgenera or the description of several new subgenera to avoid paraphyletic taxa. However, as we only studied mitochondrial (mt)DNA, introgression, incomplete lineage sorting, and insufficient resolution might influence the discrepancy between the molecular phylogeny and the subgeneric taxonomy (Toews & Brelsford, 2012).

The two main clades of *Sphingonotus* are species-rich and each of them comprises one group of little differentiated species, which are phylogenetically not completely resolved (Fig. 1). One of these radiations is found within the subgenus *Sphingonotus* (*S. caerulans*-group), the other one within the subgenus *Neosphingonotus* (*S. azurescens*-group, Hochkirch & Husemann, 2008). It was not possible to completely separate all species based upon the studied loci (ND5, 12S rRNA), although ND5, in particular, is known to be among the most variable mitochondrial genes in Orthoptera (Hochkirch, 2001). The *S. caerulans*-group includes the species *S. caerulans* (Linnaeus, 1767), *S. lluciapomaresi* (Default, 2005), *S. corsicus* Chopard, 1923, *S. willemsei* Mistshenko, 1937, *S. rubescens*, *S. gypsicola* Llucià-Pomares, 2006, and *S. lusitanicus* Ebner, 1941 comb. rev. The genetic relationships within this group were not fully resolved, possibly due to the small genetic distances between the clades (e.g. mean p-distance between *S. rubescens* and *S. gypsicola*: 0.007; between *S. lusitanicus* comb. rev. and *S. lluciapomaresi*: 0.005). *Sphingonotus caerulans* turned out to be polyphyletic with three mitochondrial lineages. Although the exact position of two of these lineages was weakly supported, it is noteworthy that specimens from the Iberian Peninsula, France, and the Balears branched together with *S. gypsicola* from Spain [posterior probability (PP) 99], with the specimens of *S. gypsicola* being nested within this branch. These two species branched together with the widespread species *S. rubescens* and the North African subspecies *S. caerulans atlas* Chapman, 1938 (PP 100). Specimens from the type

locality (Nuremberg, Germany) and other parts of Central and northern Europe, subspecies *S. caerulans caerulans* and *S. caerulans cyanopterus* (Charpentier, 1825), turned out as the sister clade to *S. lluciapomaresi* and *S. lusitanicus* comb. rev. from Iberia (although only weakly supported). The mean p-distance between the *S. caerulans* clades from south-west Europe and Central Europe was highest within the *S. caerulans*-group (0.014).

The *S. azurescens*-group is more broadly defined here than in Hochkirch & Husemann (2008). It consists of the species *S. finotianus*, *S. fuerteventuræ* Husemann, 2008, *S. savignyi*, *S. canariensis* Saussure, 1884, *S. pachecoi* (Bolívar, 1908), *S. morini*, *S. sublaevis* (Bolívar, 1908), *S. tricinctus*, and *S. azurescens*. Similar to the *S. caerulans*-group our phylogenetic analysis could not completely resolve the relationships among these taxa. This was particularly true for *S. azurescens*, *S. morini*, and *S. tricinctus*. The discrimination of *S. morini* and *S. azurescens* is rather difficult and based upon our morphometric analysis (see below) intermediate phenotypes occur (including a specimen used in our molecular study: No. 336). This might be explained by hybridization in a contact zone between both taxa with *S. morini* in the east and *S. azurescens* in the west of the Iberian Peninsula. PPs within the group were low, except for *S. pachecoi* from Lanzarote, which was resolved as a well-supported monophyletic clade. Two specimens of *S. azurescens* and *S. morini* branched off within *S. finotianus*, suggesting introgression. Nearly all taxa in the *S. azurescens*-group are assigned to the subgenus *Neosphingonotus* based upon their specialized stridulatory apparatus: thickened cross veinlets between radius and media (Hochkirch & Husemann, 2008). However, *S. savignyi* cannot be clearly grouped into any of the existing subgenera, as specimens may possess either a serrate intercalary vein (but with much stronger serration than in typical *Sphingonotus* species) or the *Neosphingonotus* stridulatory apparatus. Some specimens even possess both characters. Indeed, even specimens of *S. azurescens* may sometimes possess a weak serration of the intercalary vein in addition to the typical *Neosphingonotus* stridulatory mechanism. In females, the stridulatory apparatus is often only little developed.

The sister clade to the *S. azurescens*-group has much longer terminal branches and includes *S. almeriense* sp. nov. from southern Spain (Cabo de Gata-Nijar), *S. imitans* comb. rev. Brunner von Wattenwyl, 1882, and *S. nodulosus* sp. nov. from the southern part of the Iberian Peninsula. While *S. almeriense* sp. nov. and *S. nodulosus* sp. nov. possess the *Neosphingonotus* stridulatory mechanism, *S. imitans* comb. rev. has a serrated intercalary vein and is morphologically generally closer to *S. candidus* Costa, 1888

than to *Neosphingonotus* species. However, all three species in this clade possess a rather long male supra-anal plate compared with other species (Fig. 8A, B, G, J). *Sphingonotus lucasii* Saussure, 1888 from North Africa showed a clear sister-group relationship to *S. eurasius* Mistshenko, 1936 collected from the island of Lampedusa (Italy). The most ancient splits within the *Sphingonotus* clade were those of *S. guanchus* (Johnsen, 1985) from Gran Canaria and the two *Parasphingonotus* species *S. radioserratus* Johnsen, 1985 from North Africa and *S. femoralis* Uvarov, 1933 from Niger.

MULTIVARIATE MORPHOMETRICS OF *S. AZURESCENS* (RAMBUR, 1838) AND *S. MORINI* (DEFAUT, 2005)

The PCA showed a clear differentiation of *S. azurescens* and *S. morini* without any overlap between both species (plot not shown). The sexes were separated on the first axis (explaining 75.4% of the total variance), whereas the species were separated on the second axis (explaining 12.8% of the variance). While the first function was mainly explained by body size, the second function was mainly explained by the dimensions of the cerci and the wing band. In the

stepwise discriminant analysis, 32 individuals had to be excluded due to missing variables (as well as the three unidentified males). Nine characters were included in the stepwise discriminant analysis in the following order: (1) cerci length, (2) body length (from tip of vertex to end of tegmen), (3) minimum intraocular distance, (4) length of subocular furrow, (5) mid tegmen width (measured at end of median area), (6) anterior tegmen width (measured at precostal lobe), (7) maximum cerci width, (8) hind femur length, and (9) continuity of wing band. The first function of the discriminant analysis explained 83.1% of the variance, while the second axis explained 16.1% (Fig. 2). Wilks Lambda reached an exceptionally low value of 0.002 ($F_{27,495} = 151.1$, $P < 0.001$), illustrating a high discriminating power of the functions. Cerci length [standardized canonical discriminant coefficient (SCDC): 1.04] and body length (SCDC: -0.67) contributed most to the first discriminant function (separating sexes), while the second function was mainly explained by mid tegmen width (SCDC: 1.10), minimum intraocular distance (SCDC: -0.96), and anterior tegmen width (SCDC: -0.85) and separated the species. The posterior classification test correctly assigned all 198 specimens for which data for these

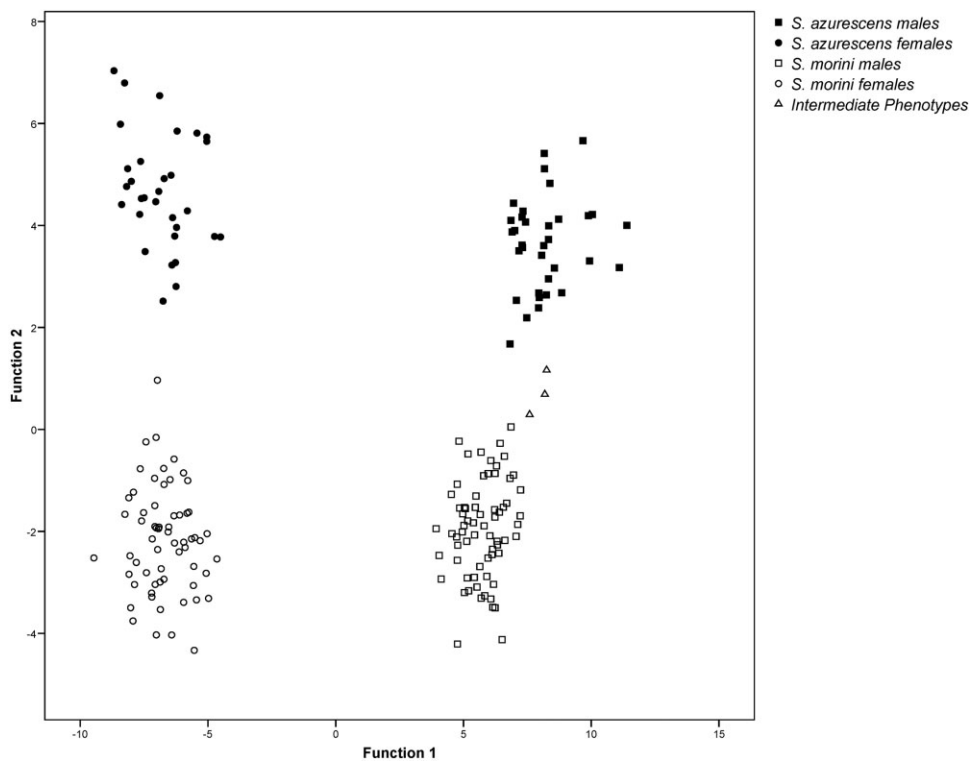


Figure 2. Plot of the first two functions of the discriminant analysis for *S. azurescens* and *S. morini*. The first function explains 83.1% of the variance (separating sexes), and the second function explains 16.1% of the variance (separating species). All individuals were classified correctly. Three individuals with intermediate phenotypes (open triangles) stem from the contact zone of both species: Castaras (Granada) and Magán (Toledo).

nine variables were available (15 individuals had to be excluded due to missing data). Two of the three individuals with unknown identity (both from Castarás, Granada) were assigned as *S. azurescens*, and one (from Magán, Toledo) as *S. morini*.

Although *S. morini* and *S. azurescens* were genetically not monophyletic, the clear morphometric differentiation of *S. azurescens* and *S. morini* supports their species status. The characters identified in the stepwise discriminant analysis as being most important are generally not in line with the original description of *S. morini* by Defaut (2005c). Defaut (2005c) also mentions a different coloration of the hind tibiae, which is greenish-white in *S. morini* (at least on the inner side close to the apex) and bluish in *S. azurescens*. However, it should be noted that the material studied by Defaut (2005c) mainly stemmed from the eastern part of the Iberian Peninsula, except for two Portuguese specimens, for which Defaut (2005c) already mentioned biometric anomalies (larger body size). Indeed, our analysis (including material from the type localities of both species) suggests that *S. azurescens* is restricted to the western half of the Iberian Peninsula, while *S. morini* is found in the eastern half. Our data also revealed that *S. azurescens* is generally larger in body size (VT males: 24.3–30.8 mm, females: 31.2–40.4 mm) than *S. morini* (males: 19.4–25.6 mm, females: 26.3–32.6 mm) and that the wing band is darker and continuous in *S. azurescens*, while it is often interrupted in *S. morini*. Furthermore, the tegmen of *S. azurescens* are slightly widened to the apex of the median area (particularly in the females), while in *S. morini* the greatest width is found at the precostal lobe. Although relatively variable, the number of secondary branches of the radial sector is greater in males of *S. azurescens* (75% have three branches, 16.7% have four branches) than in males of *S. morini* (71% have two branches, 29% have three branches and none has four branches).

Virtually all specimens of *S. azurescens* (both sexes) have a rather constant black-brownish wing fascia with well-defined margins, which is slightly diffuse in the area of the vena dividens and reaches from the anterior margin to V12 (in males V12–V14, in females V12–V15). In *S. morini* the wing fascia is variable, particularly in its extent (in males V10–V14, in females V7–V14). In 84.6% of the females and 50% of the males the wing band is interrupted and the margins are also frequently irregular or poorly defined, and the colour is less contrasting (usually brownish). In numerous specimens (particularly females), the wing band is diffuse or barely visible, sometimes even completely missing. However, in two populations (Delta del Ebro, Tarragona; Mora, Toledo) both sexes possess a strongly contrasting black-

brownish wing band. The variability of the wing fascia is a key to past erroneous taxonomic interpretations of the Iberian *Sphingonotus azurescens*-group. For example, Defaut (2005a) indicates that the wing band is discontinuous in the majority of female *S. azurescens*, while the opposite seems to be true. Furthermore, various authors (e.g. Chopard, 1943; Harz, 1975; Pardo, Gómez & Del Cerro, 1991) use exactly this trait for distinguishing *S. azurescens* from *S. arenarius* (Lucas, 1846), a North African species that erroneously had been recorded from the Iberian Peninsula. *Sphingonotus morini* and *S. arenarius* have a similar wing fascia, but they can be separated by the shape of the head, which is more robust in *S. morini*.

A character that has been frequently used to identify *Sphingonotus* species is the ratio of eye length to vertex width. Defaut (2005c) also used this ratio to distinguish *S. morini* from *S. azurescens*. Our own biometric measurements show that both species strongly overlap in this ratio. Nevertheless there are significant intraspecific differences in the overall shape of the head: in *S. azurescens* the head is higher and narrower in relation to the body size than in *S. morini*. This is reflected by the fact that the minimum intraocular distance was one of the most important characters distinguishing both species in the discriminant analysis. Based on the ratio between the minimum intraocular distance and either length of the subocular furrow, hind femur length, maximum width of the supra-anal plate, or cerci length all males of both species can be identified correctly. However, in females the overlap is greater.

Another character, which has been suggested to be of value by Defaut (2005a), is the coloration of the hind tibiae. Our data show that there is considerable variation in this trait, although each species seems to have its own tonal spectrum. In *S. azurescens* bluish colours dominate both in the basal colour as well as in the rings, although the latter can also differ in colour (e.g. turquoise, yellowish, whitish, and brownish to a much lesser extent). In *S. morini* the pattern is much more variable with three main types of coloration: (1) greenish (coastal zone from Almería to Huesca and Monegros), (2) brownish (Ebro valley), and (3) turquoise to blue-turquoise (widespread). In the third case, individuals often possess one or two blue rings, so that substantial overlap between both species occurs.

Our study shows that the male supra-anal plate is of particular taxonomic value in the genus *Sphingonotus* (see below). However, this is only partly true for the two species under consideration. In both species it is wider than long (1.19–1.65× wider than long in *S. azurescens*, 1.02–1.42× in *S. morini*), but the shape is pentagonal in *S. azurescens* (Fig. 8C–C''),

while it is more or less triangular in *S. morini* (Fig. 8D–D''), particularly in the southern part of its range (i.e. Almería, Murcia, Granada). Unfortunately, this difference is not very constant and intermediate phenotypes occur. So, its taxonomic use is limited and the trait needs to be combined with others. The same applies also to the shape of the male cerci, which are generally cylindrical, but longer in *S. azurescens* (Fig. 9C) than in *S. morini* (Fig. 9D), giving them a more robust appearance in *S. morini*. In contrast to other taxonomic studies (e.g. Mistshenko, 1936; Chopard, 1943; Aguirre & Pascual, 1987) we found no significant taxonomic value of the sculpture of the female ovipositor valves. It should be noted that in both species the valves are practically smooth, while in *S. lluciapomaresi* and *S. gypsicola* they are rugose, indicating that *S. azurescens* might have been confused with one of these species. In females, the shape of the subgenital plate is (together with the tegmina and the dark wing band) probably the best character distinguishing both species. In *S. azurescens* the apical part of the plate is bilobate, with a deep medial excision in the shape of a 'V' (Fig. 9O–O'), whereas in *S. morini* the posterior margin is concave and only weakly excised (Fig. 9P–P').

DESCRIPTION OF *SPHINGONOTUS*
(*NEOSPHINGONOTUS*) *ALMERIENSE* SP. NOV.
LLUCIÀ-POMARES

Material studied:

Type series: Holotype: ♂, Spain, Almería, Parque Natural Cabo de Gata-Níjar, Retamar, near playa de Torre García, 30SWF6376, 22 m asl, 11.viii.2009, Llucià-Pomares & Íñiguez *leg.*

Depository: MNCN

Paratypes (2♂♂ and 6♀♀): all from Spain, Almería, Parque Natural Cabo de Gata-Níjar; 2♂♂ and 4♀♀ collected near playa de Torre García, Retamar, 30SWF6376, 22 m asl, 11.viii.2009, D. Llucià Pomares & J. Íñiguez *leg.*; 1♀, road from Retamar to Cabo de Gata, 30SWF6476, 20 m asl, 30.vii.2005, J. Íñiguez *leg.*; 1♀ Salinas del Cabo de Gata, 30SWF6969, 11.x.2005, A. Hochkirch *leg.*

Depository: 2♀♀ MNCN; 1♂ and 1♀ NHM; 1♀ MCNB, 1♀ DBTU, 1♂ and 1♀ col. Llucià-Pomares (Barcelona, Spain).

Type locality

Surroundings of Playa de Torre García, Retamar, Parque Natural de Cabo de Gata (Spain: Almería).

Description of male

General facies: Habitus slender (Fig. 3); medium size compared with other Iberian species; total length from fastigium of vertex to end of tegmina 21.3–

21.9 mm (holotype: 21.4 mm), to end of hind knee 15.5–15.6 mm (holotype: 15.6 mm; Table 1).

Coloration: Coloration distinct, but variable as in other Oedipodinae, which are often homochromic with the substrate coloration. Dorsal part of head, pronotum, and first third of tegmina darker, usually brownish to reddish-brown; rest of body paler, grey to grey-brownish (Fig. 3).

Pubescence: Short and dispersed, appearing as single hairs, but denser and longer at lateral margins of mesosternum (Fig. 4C) and apical part of the abdomen, particularly at apex of subgenital plate and cerci (Fig. 4D).

Head: Eyes only little longer than wide (Fig. 4A, B), length to width ratio: 1.15–1.22 (holotype: 1.15; Table 2). Vertex strongly narrowed between eyes (Fig. 4A), minimum width 0.64–0.69 mm (holotype: 0.64), ratio of eye length to vertex width very narrow (2.29–2.55; holotype: 2.29); fastigium of vertex slightly depressed in centre, maximum width twice its length (Fig. 4A); median carinula faintly visible, little developed, and dorsally rounded; lateral carinulae well marked over whole course, mostly on the same level as eyes, upper part subangular to rounded. Fastigial foveolae poorly defined, subtriangular or trapezoidal, only slightly excised, margins indistinct and rounded, except for inner part, which is slightly bulging, slightly larger than lateral ocelli. Frontal ridge slightly depressed, moderately widened at level of median ocellus; upper third of lateral carinulae little developed, slightly converging or subparallel; median third thickened; lower third little developed and diverging, not reaching clypeo-frontal suture. Subocular furrow little incised and slightly sinuous, length *c.* 3/4 of eye length (ratio eye length/length of subocular furrow = 1.33–1.38; holotype: 1.37). Maxillary and labial palps whitish with cylindrical limbs, except terminal limbs, which are moderately globose at apex. Antennae filiform (Fig. 4A), 25–26 segments in addition to scape; ringed, particularly in two basal thirds, alternating dark and pale brown segments; relatively short, between 5.8 and 5.9 mm (holotype: 5.9 mm), 1.09–1.18 times longer than head and pronotum together (holotype: 1.18×) and *c.* 0.7 times hind femur length.

Pronotum: Pronotal disc 2.95–3.28 mm long (holotype: 2.95 mm) and *c.* 1.2 times longer than wide (Fig. 4A); colour pattern characteristic and rather constant, densely dark-brownish speckled in median zone with two broad pale, contrasting bands running parallel to lateral carinae; integument slightly rugose, without tubercles, groins, or callosities. Anterior margin

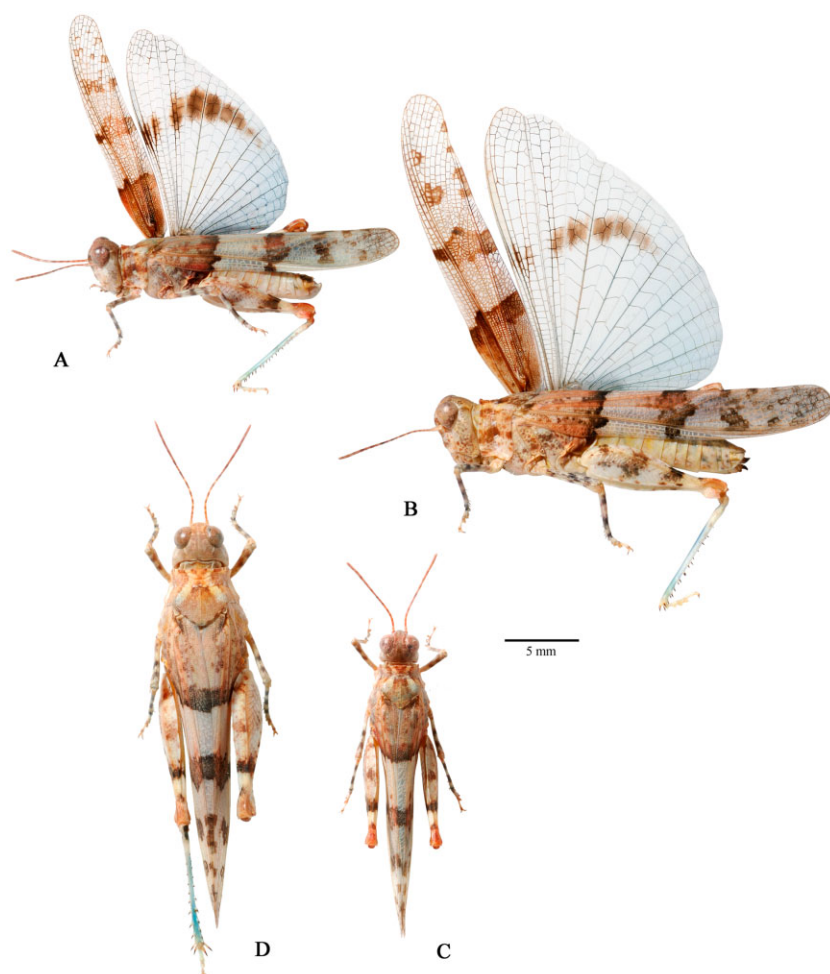


Figure 3. *Sphingonotus (Neosphingonotus) almeriense* sp. nov., in lateral view and with spread wings: A, male holotype; B, female paratype, and in dorsal view: C, male holotype; D, female paratype.

slightly convex, with a very narrow and shallow median excision; hind margin rectangular, with apex rounded (Fig. 4A). Median carina well developed in anterior region of prozona, little elevated, not visible between first and posterior sulcus, well developed in metazona, decreasing in height and thickness towards apex. Median carina with three transverse sulci; anterior and median sulcus parallel curved and moderately separated, median and third sulcus strongly approximated in central part, with two small tubercles in between and on both sides of median carina (Fig. 4A); first sulcus crosses median carina behind half of prozona; posterior sulcus situated way ahead of middle of pronotum; metazona 2.14–2.21 times longer than prozona (holotype: 2.14). Anterior part of prozona moderately tectiform. Paranota 1.3–1.4 times higher than long; submarginal sulcus not reaching median carina (Fig. 4B); anterior margin slightly concave, posterior margin straight and slightly oblique; lower margin sinuous; lower anterior

and posterior angle rounded and without any projection, never forming a denticle (Fig. 4B).

Sternum: Sternal plate slightly wider than long (Fig. 4C); mesosternum whitish and grossly spotted, rest smooth and yellowish; mesosternal interspace 1.41–1.51 times wider than long (holotype: 1.41) (measured according to Llorente & Presa, 1997); metasternal interspace 1.62–1.75 times wider than long (holotype: 1.62); both interspaces clearly defined by deep sulci, which separate the meso- and metasternum.

Legs: Hind femora (Fig. 3A) 8.1–8.4 mm long (holotype: 8.2), moderately robust, 3.55–3.81 times longer than wide (holotype: 3.81); external side greyish or beige, partly or completely traversed by three dark brownish bands, pre-apical band complete and distinct, the other two situated near mid and close to the base more or less incomplete and less contrasting, in

Table 1. Morphometric measurements of *Sphingonotus almeriense* sp. nov. and *Sphingonotus noctulosus* sp. nov. (Holotype – min – (mean) – max (mm))

Trait	<i>S. almeriense</i> males (N = 3)	<i>S. almeriense</i> females (N = 6)	<i>S. noctulosus</i> males (N = 11)	<i>S. noctulosus</i> females (N = 5)
Total length vertex to apex of the tegmen (V-T)	21.4–21.3–(21.5)–21.9	25.4–(27.0)–28.5	20.7–19.8–(20.9)–22.0	24.6–(26.5)–27.9
Total length vertex to hind knee (V-hK)	15.6–15.5–(15.5)–15.6	19.1–(19.7)–21.3	15.1–14.5–(15.3)–16.2	18.4–(19.6)–20.6
Distance hind knee/apex of the tegmen (hK-T)	5.8–5.8–(6.0)–6.3	6.3–(7.3)–8.3	5.6–5.0–(5.6)–6.3	5.9–(6.9)–7.8
Total length vertex to apex of subgenital plate (V-sP)	16.7–16.4–(16.7)–17.1	19.1–(20.4)–22.0	15.1–14.8–(15.5)–16.3 (N=8)	20.8–(20.9)–21.0 (N=2)
Length of antenna (LAnt)	5.9–5.8–(5.8)–5.9	7.3–(7.5)–7.8 (N = 3)	6.4–5.9–(6.3)–6.7	6.8–(6.9)–7.2 (N = 4)
No. of flagellar segments of antenna	26–25–(25.7)–26	25–(25.8)–26	23–23–24–25 (N = 7)	25 (N=2)
Length of metazonal disc in midline (LMtz)	2.01–2.01–(2.12)–2.25	2.55–(2.76)–2.92	1.90–1.82–(1.93)–2.05	2.30–(2.55)–2.68
Length of pronotal disc in midline (LPPrz)	0.94–0.94–(0.97)–1.03	1.17–(1.21)–1.27	0.93–0.90–(0.95)–1.05	1.15–(1.19)–1.25
Length of pronotal disc in midline (LP)	2.95–2.95–(3.09)–3.28	3.73–(3.97)–4.10	2.83–2.72–(2.88)–3.10	3.45–(3.74)–3.85
Total length head and pronotum (LP+LH)	4.9–4.9–(5.1)–5.3	6.5–(6.8)–7.1 (N = 5)	4.80–4.65–(4.86)–5.10	5.60–(6.18)–6.50
Tegmen length (LT)	17.1–17.0–(17.1)–17.3	20.2–(21.5)–22.5	16.4–16.10–(16.9)–17.7	20.3–(21.6)–22.6
Max. tegmen width (WT)	3.0–3.0–(3.1)–3.2	3.4–(3.8)–4.1	2.97–2.68–(2.89)–2.97	3.28–(3.57)–3.76
Length of medial area (LMA)	8.8–8.4–(8.6)–8.8	9.9–(10.7)–11.4	8.6–8.2–(8.9)–9.7	10.4–(11.2)–11.8
Length of hind wing (LW)	15.7–15.7–(15.9)–16.1	18.8–(20.3)–21.1	15.1–14.5–(15.5)–16.3	18.3–(20.1)–21.3
Max. hind wing width (WW)	9.3–9.3–(9.7)–9.9	10.7–(11.9)–12.9	8.6–8.0–(8.7)–9.5	10.4–(11.2)–11.8
Min. vertex width (wV)	0.64–0.64–(0.67)–0.69	0.84–(0.88)–0.90	0.69–0.56–(0.64)–0.69	0.82–(0.84)–0.86 (N = 4)
Min. interocular distance (iO)	0.70–0.65–(0.68)–0.70	0.86–(0.90)–0.93	0.70–0.56–(0.64)–0.70	0.84–(0.86)–0.88 (N = 4)
Eye length (LE)	1.58–1.58–(1.62)–1.65	1.73–(1.88)–1.98	1.55–1.53–(1.57)–1.63	1.50–(1.67)–1.77
Max. eye width (WE)	1.37–1.35–(1.37)–1.38	1.48–(1.56)–1.63	1.28–1.27–(1.31)–1.36	1.30–(1.38)–1.44
Length of sub-ocular furrow (LSO)	1.15–1.15–(1.19)–1.23	1.50–(1.61)–1.77	1.12–1.12–(1.19)–1.25	1.48–(1.65)–1.80
Hind femur length (LF)	8.2–8.1–(8.2)–8.4	9.7–(10.3)–10.8	7.6–7.6–(8.0)–8.7	9.6–(10.3)–10.7
Max. hind femur width (WF)	2.15–2.15–(2.24)–2.30	2.75–(2.88)–3.00	2.13–1.95–(2.08)–2.18	2.57–(2.67)–2.76 (N = 4)
Min. width of mesosternal interspace (wMs)	1.10–1.05–(1.08)–1.10	1.53–(1.66)–1.78	1.00–1.00–(1.14)–1.25	1.46–(1.57)–1.65
Length of mesosternal interspace (LMs)	0.78–0.73–(0.75)–0.78	0.95–(1.05)–1.10	0.73–0.73–(0.78)–0.85	0.96–(1.13)–1.23
Width of metasternal interspace (WMT)	0.86–0.86–(0.90)–0.93	1.22–(1.40)–1.50	0.95–0.88–(0.94)–1.06	1.40–(1.52)–1.68
Length of metasternal interspace (LMt)	0.53–0.53–(0.53)–0.54	0.70–(0.79)–0.90	0.45–0.38–(0.44)–0.50	0.58–(0.62)–0.66
Length of male supra-anal plate (LSa)	1.14–1.13–(1.14)–1.16	–	1.10–1.06–(1.14)–1.21	–
Max. width of male supra-anal plate (WSa)	0.86–0.85–(0.88)–0.92	–	1.03–1.03–(1.07)–1.14	–
Cercus length (LC)	0.79–0.78–(0.79)–0.80	0.51–(0.54)–0.56 (N = 5)	0.75–0.64–(0.72)–0.78	0.34–(0.44)–0.51
Max. cercus width (WC)	0.54–0.49–(0.51)–0.54	0.39–(0.40)–0.41 (N = 5)	0.40–0.36–(0.39)–0.43	0.28–(0.30)–0.33
Length of apical valves of ovipositor (LVv)	–	0.64–(0.69)–0.71 (N = 5)	–	0.56–(0.65)–0.73
Max. width of apical valves of ovipositor (WVv)	–	0.38–(0.40)–0.45 (N = 5)	–	0.38–(0.43)–0.47
No. of thickened cross veinlets between R & M	8–7–(8)–9	5–(7.8)–11	14–11–(12.9)–16	11–(15.4)–18
Mean distance between cross veinlets betw. R & M	0.39–0.32–(0.36)–0.39	0.31–(0.43)–0.71	0.21–0.19–(0.25)–0.31	0.19–(0.24)–0.27
No. of secondary branches of radial sector vein (nRS)	2–2 (2x)–3 (1x)	2 (4x)–3 (1x)	2–2 (9x)–1 (2x)	2 (4x)–3 (1x)
Spines of the posterior tibiae (internal margin)	11/11–11–(10.5)–10 (N=6)	9–(10.3)–11 (N = 12)	11/11–10–(11.0)–12 (N=20)	11–(11.1)–12 (N=8)
Spines of the posterior tibiae (outer margin)	8/8–8–(8)–8 (N = 6)	7–(7.8)–8 (N = 12)	8/8–7–(8.2)–9 (N = 20)	7–(7.8)–8 (N = 8)
Posterior end of dark wing band (vannal vein no.)	8–8 (2x)–10 (1x)	7 (5x)–8 (1x)	10–10 (6x)–11 (4x)–12 (1x)	10 (1x)–11 (2x)–12 (2x)

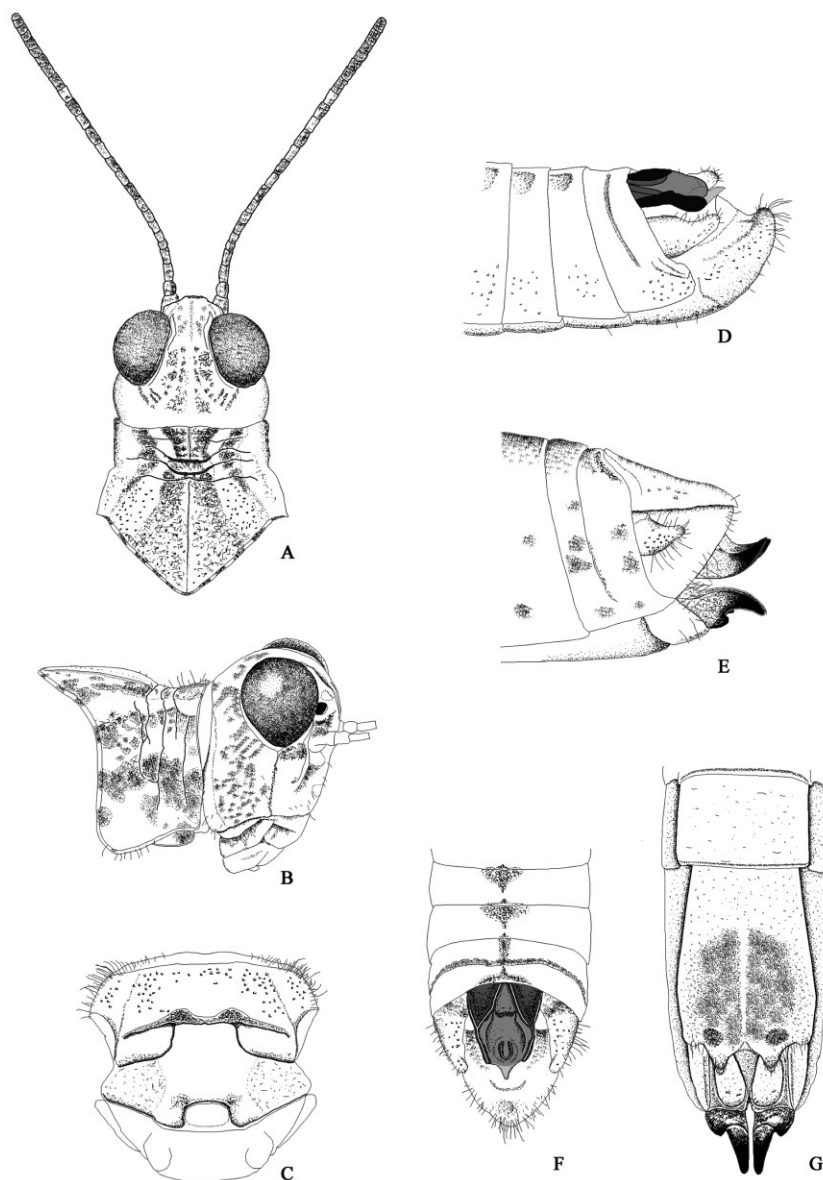


Figure 4. Main characters of male and female of *SpHINGONOTUS* (*NeosPHINGONOTUS*) *almeriense* sp. nov.: A, head and pronotum of male holotype in dorsal view; B, head and pronotum of male holotype in lateral view; C, meso- and metasternum of male holotype; D, end of male abdomen in lateral view (holotype); E, end of female abdomen in lateral view (paratype); F, end of male abdomen in dorsal view (holotype); G, end of female abdomen in ventral view (paratype).

some cases only apparent on upper carinula and upper carina of hind femur; first and third band situated at same position as transverse tegminal bands; inner side of hind femur brownish, with a pre-apical dark transverse band and a broad whitish apical band which contrasts strongly to the first one. Hind knees with reddish-brown upper genicular lobe, lower lobe paler. Hind tibiae (Fig. 3A) with 7–8 external spines (8/8 in holotype) and 10–11 internal spines (holotype: 11/11); base of spines whitish, reflecting bluish, with dark brown apices; inner apical spurs

longer than pre-apical spurs, both yellowish at the base and apically similarly coloured as spines. Outer side of tibiae basally dark brown followed by a whitish pre-basal ring, turning gradually azure bluish towards apex, with strongest intensity in central part, apical part greenish-blue. Arolium longish, *c.* three times longer than wide.

Wings: Tegmen 5.4–5.7 times longer than wide (holotype: 5.7), surpassing hind knees considerably (5.8–6.3 mm; holotype: 5.8 mm; Fig. 3A); reddish brown in

Table 2. Main biometric ratios of *Sphingonotus almeriense* sp. nov. (three males and six females) and *Sphingonotus nodulosus* sp. nov. (11 males and five females); **Holotype** – min – (mean) – max. For abbreviations see Table 1

Biometric ratio	<i>S. almeriense</i> males (<i>N</i> = 3)	<i>S. almeriense</i> females (<i>N</i> = 6)	<i>S. nodulosus</i> males (<i>N</i> = 11)	<i>S. nodulosus</i> females (<i>N</i> = 5)
LAnt/LF	0.72 –0.69–(0.71)–0.72	0.72–(0.73)–0.74	0.84 –0.71–(0.81)–0.86	0.65–(0.66)–0.71
LAnt/(LP+LH)	1.18 –1.09–(1.14)–1.18	1.10–(1.12)–1.15	1.33 –1.22–(1.29)–1.34	1.10–(1.14)–1.21
LF/WF	3.81 –3.55–(3.67)–3.81	3.47–(3.56)–3.66	3.57 –3.57–(3.86)–4.14	3.72–(3.81)–3.96
LT/WT	5.7 –5.4–(5.6)–5.7	5.44–(5.67)–5.94	5.52 –5.52–(5.81)–6.08	5.78–(6.04)–6.19
LW/WW	1.69 –1.63–(1.65)–1.69	1.64–(1.70)–1.77	1.72 –1.61–(1.77)–1.92	1.76–(1.80)–1.87
LMtz/LPrz	2.14 –2.14–(2.18)–2.21	2.16–(2.29)–2.47	2.04 –1.95–(2.02)–2.12	2.00–(2.14)–2.31
LE/wV	2.29 –2.29–(2.42)–2.55	1.94–(2.15)–2.29	2.25 –2.25–(2.48)–2.75	1.83–(1.97)–2.06
LE/iO	2.26 –2.26–(2.38)–2.51	1.90–(2.08)–2.23	2.21 –2.21–(2.45)–2.75	1.79–(1.93)–2.01
LE/LSo	1.37 –1.33–(1.36)–1.38	1.08–(1.17)–1.24	1.38 –1.28–(1.33)–1.38	0.98–(1.01)–1.06
LE/WE	1.15 –1.15–(1.18)–1.22	1.17–(1.20)–1.24	1.21 –1.19–(1.21)–1.23	1.15–(1.20)–1.23
wMs/LMs	1.41 –1.41–(1.45)–1.51	1.48–(1.58)–1.66	1.37 –1.32–(1.46)–1.57	1.24–(1.39)–1.52
WMt/LMt	1.62 –1.62–(1.69)–1.75	1.61–(1.78)–2.06	2.11 –1.88–(2.13)–2.43	2.32–(2.43)–2.67
LSa/WSa (males)	1.33 –1.26–(1.31)–1.33	–	1.07 –1.01–(1.06)–1.11	–
LC/WC	1.46 –1.46–(1.54)–1.59	1.28–(1.33)–1.37	1.88 –1.61–(1.83)–2.03	1.21–(1.44)–1.70
LVv/WVv (females)	–	1.58–(1.67)–1.82	–	1.47–(1.52)–1.56

basal quarter, which is densely reticulated; the rest faintly grey, except for unpigmented apex (Fig. 3A). Fore wings with three transverse bands: first band at end of basal third, continuous and obscure reddish brown, strongly contrasting; second band situated midway slightly paler; third band at beginning of last third with similar colour as second band but discontinuous, forming between two and five large more or less separated speckles; in subapical part of fore wing 5–7 small scattered speckles can occur, not building a fourth band. Anterior margin moderately convex in basal third; subcosta, radius and media running parallel, very close (particularly the latter two) from base almost to apex of medial area; between radius and media 7–9 thickened transverse veinlets (holotype: 8), in some cases more pronounced in contact region with radius (Fig. 7A); interval between veinlets variable (even within a single specimen), varying between 0.21 and 0.53 mm (mean: 0.36 mm; holotype: 0.39 mm); radial sector with two or three ramifications; intercalary vein smooth, without serration, almost straight or moderately curved in first three-quarters, very irregular, and interrupted in last quarter; basal part equidistantly between media and cubitus or slightly closer to cubitus; distal part closer to media; medial area extending approximately to centre of fore wing. Hind wings 1.6–1.7 times longer than wide, dark brownish fascia extending from costal margin to V8–V10 (holotype: V8, Fig. 3A), partly interrupted between cubitus and vena dividentis; wing disc pale azure with strongest intensity close to base, apically (behind fascia) hyaline; principal vannal veins dark blue or bluish brown, secondary veins and veinlets pale azure.

Abdomen: General coloration beige-yellowish, dorsally darker, ventrally in orange shade. Tympanum large, almost twice as high as wide, semi-lunar, and regularly rounded at posterior margin; sub-tympanal lobe large, occupying approximately same area as tympanal opening. Subgenital plate acutely conical (Fig. 4D), projecting slightly above supra-anal plate. Cerci short, slightly shorter than supra-anal plate, 1.5–1.6 times longer than wide, strongly thickened in basal third, abruptly narrowed in the middle (Figs 4D, 9A); distal third cylindrical, apex rounded; basal part more than twice as wide as apical part. Supra-anal plate dark brown, strongly contrasting with rest of abdominal apex, which is yellowish-orange; *c.* 1.3 times longer than wide (Figs 4F, 8A, A'); basal and apical lobes poorly developed, laterally only slightly expanding; lateral margins thickened and strongly sclerotized, converging gently and running regularly almost to apex; internal carinae of basal part with its proximal ends next to each other at anterior margin of supra-anal plate; transverse carina short and situated at end of basal third; basal internal carinae and transverse carina forming a characteristic 'A'-shape (Fig. 8A, A'); interlobular apical space smooth and strongly concave; internal apical carina close to apex, forming a 'U' and encompassing a small elongated depression; apex slightly sclerotized, semi-membranous, and forming a small acute tooth which is moderately projecting.

Genitalia: Epiphallus twice as wide as long (Fig. 10A); ancorae very close, slender, slightly inclined, and incurved, distance between apices in holotype

0.19 mm; bridge short and wide; external margins of lateral plates concave, lateral projections large, posterior projections flattened, and angulate, anterior projections thickened and rounded; lophi small, bipartite, internal part slightly shorter than external part, kidney-shaped, and oriented slightly oblique, external part transverse.

Description of female

Habitus similar to male, but body larger and stouter (Fig. 3B, D); total length from fastigium of vertex to end of tegmina 25.4–28.5 mm, to end of hind knee 19.1–21.3 mm.

Furthermore, the female differs from the male in the following characters:

Vertex width and minimum interocular distance proportionally greater, ratio between eye length and these two parameters varies between 1.94 and 2.29 (mean 2.15) and between 1.90 and 2.23 (mean 2.08), respectively.

Mesosternal interspace proportionally wider, ratio between minimum width and length 1.48–1.66 (mean 1.58).

Transverse band of hind wings less contrasting (Fig. 3B), paler and more diffuse; interrupted between costal margin and vena *dividens*; in some specimens indistinguishable in this zone or between costa and V1, in these cases only indicated by a dark coloration of the corresponding veins; generally the wing band reaches distally V7 (V8 in a single specimen).

Transverse veinlets between radius and media distinctly thickened, interval between veinlets greater than in males (mean: 0.43 mm), number of veinlets extremely variable (between five and 11) as well as mean interval between them (0.31–0.71 mm).

Subgenital plate (Fig. 4G) slightly more than twice as long as 7th sternite (mean: 2.12 \times); distal region partially coriaceous, more extensive near posterior margin, which is deeply and widely subtriangular or semicircular excised, bordered by two sclerotized extensions, with apex rounded or subangular (Fig. 4G).

Cerci similar to male, but shorter and more robust, distal part shorter, 1.3–1.4 times longer than wide (Fig. 9G).

Apical valves of ovipositor in ventral view strongly narrowed and divided by a transverse carina, 1.6–1.8 times longer than wide (Fig. 4G); hind margin of proximal part strongly convex, forming a robust tooth; distal part slender, *c.* 2.5 times longer than wide and 1.5 times longer than proximal part, blackish except for base; apex regularly rounded; basal valves (Fig. 4G) generally smooth and without apparent callosities, length similar to the apical valves.

Etymology

The epithet is derived from the name of the province and municipal Almería, from which hitherto the only records of the species exist.

DIFFERENTIAL DIAGNOSIS

Sphingonotus almeriense sp. nov. differs in the following characters from other Iberian *Sphingonotus* species. It has a specialized stridulatory apparatus (thickened cross veinlets between radius and media, Fig. 7A), which is typical for the subgenus *Neosphingonotus*. This character is not found in the majority of other Iberian *Sphingonotus* species, which belong to the subgenus *Sphingonotus*: *S. caeruleans*, *S. octofasciatus*, *S. rubescens*, *S. imitans* comb. rev., *S. lusitanicus* comb. rev., *S. lluciapomaresi*, and *S. gypsicola*. The only other *Sphingonotus* species on the Iberian Peninsula which possess the *Neosphingonotus* stridulatory organ are *S. (N.) azurescens*, *S. (N.) morini*, and *S. (N.) nodulosus* sp. nov. However, in the first two species the stridulatory apparatus is less pronounced than in the latter species. *Sphingonotus almeriense* sp. nov. also has shorter antennae compared with other Iberian species, particularly in the males; the ratio between length of antennae and length of hind femur in *S. azurescens* is 0.85–1.05, in *S. morini* 0.90–1.05 (see Defaut, 2005b), in *S. nodulosus* sp. nov. 0.71–0.86, while in *S. almeriense* sp. nov. it is 0.69–0.72.

The best characters to distinguish *S. almeriense* sp. nov. from other Iberian and North African *Neosphingonotus* species are the genitalia (cerci, male supra-anal plate, male epiphallus, and female subgenital plate). *Sphingonotus almeriense* sp. nov. and *S. nodulosus* sp. nov. are the only species in which the male supra-anal plate is longer than wide (*c.* 1.3 times in *S. almeriense* sp. nov., Fig. 8A, A'; *c.* 1.1 times in *S. nodulosus* sp. nov., Fig. 8B, B'); in all other Iberian *Neosphingonotus* species it is wider than long (generally between 0.7 and 0.8 times longer than wide; Fig. 8). Only in *S. (N.) paradoxus*, which occurs in northern Africa, it is as long as wide (Fig. 8G). However, *S. paradoxus* has a slightly yellowish basal wing disc. Another species with a supra-anal plate which is wider than long is *S. (S.) imitans* comb. rev. (Fig. 8J), but this species is easily distinguished from *S. almeriense* sp. nov. by the presence of a serrated intercalary vein and the absence of a wing band. Moreover, the transverse carina of the supra-anal plate is short and the interlobular space has a triangular form in *S. almeriense* sp. nov.; in other species the transverse carina is longer and the interlobular space is more or less rectangular to trapezoidal, but never triangular. Furthermore, the apex of the supra-anal plate is smaller, appearing semi-membranous

and slightly longer than wide; in other species the apices are always robust and wider than long (Fig. 8); in *S. nodulosus* sp. nov. it is characterized by an apical nodular process (Fig. 8B, B'). The cerci of both sexes (Fig. 9A, G) are also unique as they are strongly narrowed in the middle and proportionally shorter (in males $\leq 1.6\times$ longer than maximal width). In the other species the cerci are cylindrical in the males, in *S. nodulosus* sp. nov. regularly conical (Fig. 9B, H), and much longer than wide ($\geq 1.6\times$, often more than $2\times$; Fig. 9). Only in *S. imitans* comb. rev. the cerci are also less than two times longer than wide (Fig. 9F, L). The male epiphallus of *S. almeriense* sp. nov. differs clearly from the other species by its short and robust bridge and the small distance between the ancorae (Fig. 10A); in the other species the bridge is proportionally longer and the ancorae are more separated (Fig. 10B–J); finally, at the posterior margin of the female subgenital plate (Fig. 9M) a triangular or semicircular excision can be found, bordered by two robust near-triangular elongations with a narrow subangular apex. This character is notably different from *S. azurescens* and *S. morini*. The hind margin of the subgenital plate varies from slightly concave to straight in *S. morini* (Fig. 9P–P'). It is more variable in *S. azurescens* (Fig. 9O–O'), but never as deep as in *S. almeriense* sp. nov. and without conspicuous elongations; *S. nodulosus* sp. nov. also has a deeply excised end of the female subgenital plate, but it is narrower and delimited by two broadly rounded lobes (Fig. 9N, N').

In comparison with other North African *Neosphingonotus* species (*S. paradoxus*, *S. finotianus*, *S. tricinctus*), *S. almeriense* sp. nov. is much smaller and has shorter wings (V–T < 22.0 in males, 29.0 in females; LT < 17.5 in males, 22.5 in females). In *S. paradoxus*, *S. canariensis* and *S. azurescens* the wing band is continuous (sometimes shortly interrupted near the vena dividens), extending more to the inner margin and longer (usually extending V10), while in *S. almeriense* sp. nov. the wing band is discontinuous (interrupted between cubital vein and vena dividens) and reaches V7 in females (max. V8), maximally V10 in males. In *S. tricinctus*, the wing band is very broad, covering large parts of the basal wing disc (almost continuous to the internal margin). In *S. finotianus* the wing band is very weak, usually only visible as a dark infumation. For further discrimination of *S. almeriense* sp. nov. and *S. nodulosus* sp. nov. see also below.

DISTRIBUTION, ECOLOGY, AND BIONOMICS

So far, *Sphingonotus almeriense* sp. nov. has only been found in the Parque Natural del Cabo de Gata-Níjar (Almería, south-east Spain; Fig. 12D). All known

individuals have been collected from the coastal dune zone and the species seems to be missing further inland (in contrast to *S. morini*, which co-occurs with *S. almeriense* sp. nov.). The major part of the littoral zone near Almería, in which the P. N. del Cabo de Gata-Níjar is located, belongs to the phytogeographical Murciano-Almeriense province with a semiarid–arid Mediterranean climate. The annual rainfall is < 200 mm, but aridity is partly compensated for by coastal humidity. The dominant vegetation type is a *Zizypheto loti sigmetum* (Rivas-Martínez, 1987), a sparse halophytic bush vegetation, which can become high and dense in some places and is characterized by *Zizyphus lotus*. Furthermore, the following plant species are abundant: *Artemisia herba-alba*, *Lycium intricatum*, *Thymelaea hirsuta*, *Ballota hirsuta*, *Launaea arborescens*, *Salsola oppositifolia*, and *Lygeum spartum*. Similar to other *Sphingonotus* species, *S. almeriense* sp. nov. is terricolous and apparently strongly psammophilous in contrast to *S. morini*, which is more ubiquitous and also occurs on compacted substrates. Another peculiarity compared with its congeners is found in the flight behaviour of escaping individuals. Startle flights are quick and short, not longer than 2–3 m, while *S. morini* usually flies longer and further.

DESCRIPTION OF *SPHINGONOTUS* (*NEOSPHINGONOTUS*) *NODULOSUS* SP. NOV.

LLUCIÀ-POMARES

Material studied:

Type series: Holotype: ♂, Portugal, Leiria, Lagoa de Óbidos, Caldas da Rainya, 29SMD8063, 0 m asl, 30.viii.2011, F. Barros & P. Lemos leg.

Depository: MNCN: Paratypes (10♂♂, 5♀♀): all from Portugal, Leiria, Lagoa de Óbidos, Caldas da Rainya, 29SMD8063, 0 m asl; 5♂♂, 3♀♀, 11.vii.2004, G. Kilzer leg.; 2♂♂, 2♀♀, 26.viii.2011, F. Barros & P. Lemos leg.; 3♂♂, 30.viii.2011, F. Barros & P. Lemos leg.

Depository

1♂, 1♀ MNCN; 2♂♂, 1♀ DBTU; 1♂, 1♀ MCNB; 2♂♂, 1♀ NHM; 4♂♂, 1♀ col. Lluçia-Pomares (Barcelona, Spain).

Other material studied: 3♂♂, Portugal, Leiria, Lagoa de Óbidos, Caldas de Rainya, 11.vii.2004, G. Kilzer leg, DBTU; 1♂, same locality, 30.viii.2011, F. Barros & P. Lemos leg, DBTU (all conserved in ethanol); 1♂, Spain, Cádiz, Los Toruños, Puerto de Santa María, 29.vi.2009, J. Íñiguez leg, col. JIY; 2♂♂, 1♀, Spain, Toledo, Mora, Arroyo de los Rodados, 2.ix.2006, J. Íñiguez leg, col. JIY.

Type locality

Lagoa de Óbidos, Caldas da Rainha (Portugal: Leiria).

Description of male

General facies: Habitus slender (Fig. 5), small compared with other Iberian species; total length from fastigium of vertex to end of tegmina 19.8–22.0 mm (holotype: 20.7 mm), to end of hind knee 14.5–16.2 mm (holotype: 15.1 mm, Table 1).

Coloration: Coloration rather uniform, but with variation in hue; mainly pale, ivory white, particularly the head (except for vertex and occiput, which are brownish), prozona of pronotum, paranota, fore and mid legs, and external area of hind femora, pleural region, and medial area and apical quarter of the tegmen; metazona and basal third of tegmen reddish-

brown; tegmen with two transverse brownish-black bands, strongly contrasting, first band situated at end of the first third, second in mid; apical half of tegmen with various speckles of variable number and size; abdomen yellowish, almost orange (Fig. 5).

Pubescence: Short and dispersed, only slightly denser at inner posterior angle of paranota, dorsal carina of hind tibiae, external margin of sternal plate, cerci, and apex of subgenital plate.

Head: Eyes oval, moderately longer than wide (Fig. 6A, B); length to width ratio 1.19–1.23 (holotype: 1.21; Table 2). Occiput smooth. Vertex strongly narrowed between eyes (Fig. 6A; ratio eye length to vertex width: 2.25–2.75 (holotype: 2.25); minimum interocular distance 0.56–0.70 mm (holotype: 0.70 mm); fastigium of vertex *c.* twice as wide as long,

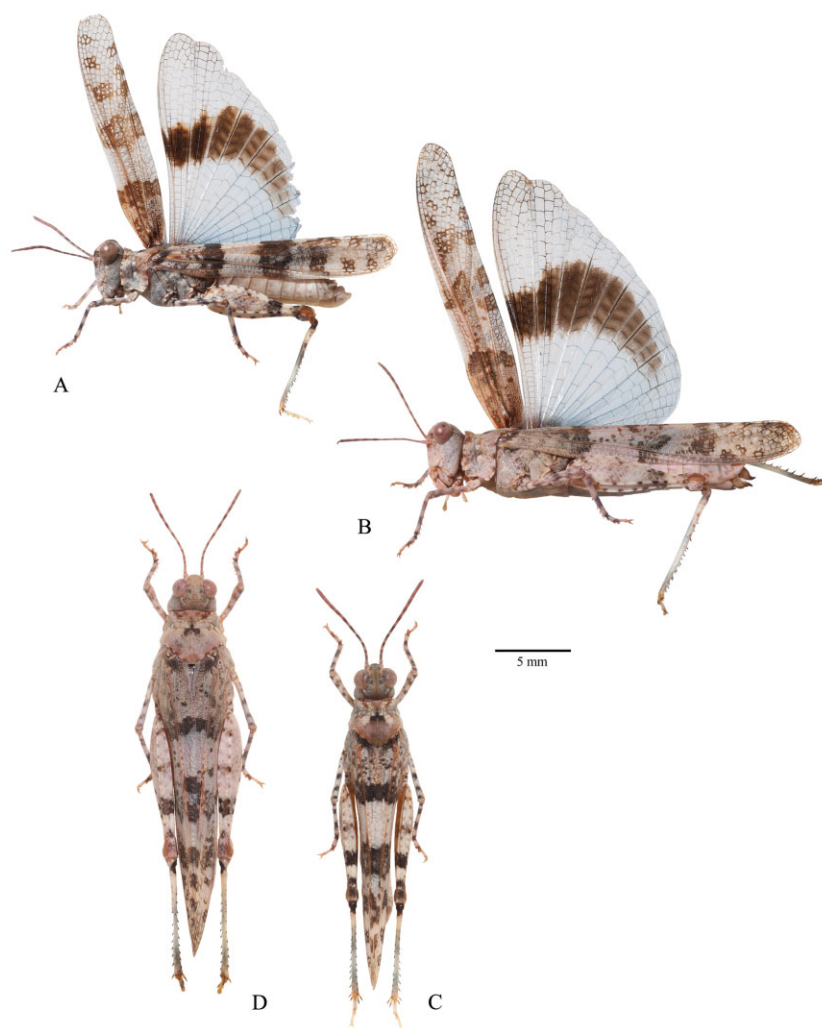


Figure 5. *Sphingonotus* (*Neosphingonotus*) *nodulosus* sp. nov., in lateral view and with spread wings: A, male holotype, B, female paratype, and in dorsal view: C, male holotype; D, female paratype.

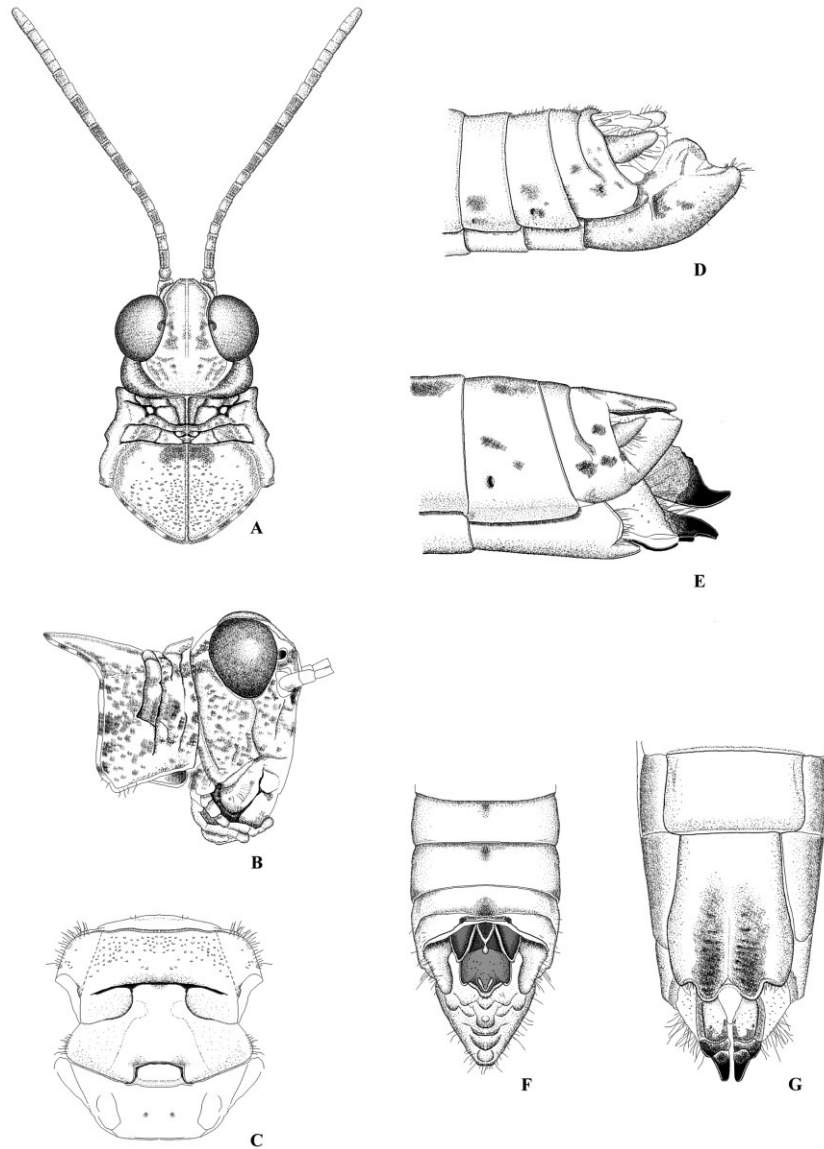


Figure 6. Main characters of male and female of *Sphingonotus (Neosphingonotus) nodulosus* sp. nov.: A, head and pronotum of male holotype in dorsal view; B, head and pronotum of male holotype in lateral view; C, meso- and metasternum of male holotype; D, end of male abdomen in lateral view (holotype); E, end of female abdomen in lateral view (paratype); F, end of male abdomen in dorsal view (holotype); G, end of female abdomen in ventral view (paratype).

apically truncate and moderately concave; carinulae variable, median carinula faintly visible, only indicated by a dark dashed line, sometimes slightly elevated; lateral carinulae always well developed (in holotype moderately high and dorsally rounded, but in other specimens considerably projecting and angular), almost laminar and partly reaching inner margin of eyes. Fastigial foveolae trapezoidal, almost invisible to strongly defined, excavated and with protruding margins (except for lower part), slightly larger than lateral ocelli. Frons in lateral view split in the middle (Fig. 6B). Frontal ridge coarsely dotted,

upper third with subparallel margins, barely diverging, and strongly projecting above median ocellus, below ocellus abruptly constricted and ventrally gradually widened with decreasing margins, which disappear close to clypeo-frontal suture. Subocular furrow broad, deep, and almost straight to slightly sinuous, shorter than eye length (ratio eye length/length of subocular furrow = 1.28–1.38; holotype: 1.38). Genae slightly convex. Antennae filiform, slightly widened in apical third (Fig. 6A), 23–24 segments in addition to scape; ringed, particularly in basal third, with alternating dark brown and pale

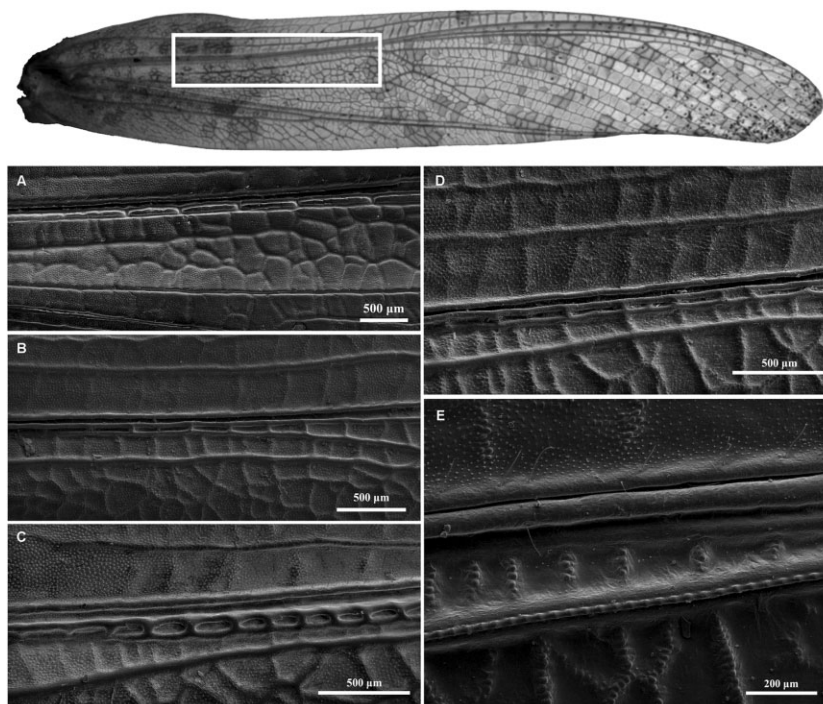


Figure 7. SEM photographs of the stridulatory organs of different *Sphingonotus* species: A, *Sphingonotus* (*N.*) *almeriense* sp. nov., B, *S.* (*N.*) *tricinctus* (Tunisia), C, *S.* (*N.*) *finotianus* (Tunisia), D, *S.* (*N.*) near *morini* (Morocco), E, *S.* (*S.*) *rubescens* (Spain, Canary Islands, La Gomera).

segments; antennal length 5.9–6.7 mm (holotype: 6.4 mm), 1.2–1.3 times longer than head and pronotum together.

Pronotum: Pronotal disc 2.72–3.10 mm long (holotype: 2.83 mm), about 1.1 times longer than wide (Fig. 6A); anterior part of prozona tectiform (variable); metazona slightly convex; anterior half of prozona and metazona brownish, posterior half pale, whitish, whitish-rose, rose or almost purple; posterior half of median carina of prozona and central part of posterior sulcus with characteristic black pattern (Fig. 6A), forming an inverted 'T' or 'Y' which fades in metazona. Paranota ivory white except for upper hind quarter, which is brownish (in one paratype with blackish and purple speckles); integument slightly rugose, appearing slightly granulose or finely spotted, but without tubercles or callosities (Fig. 6A); transverse fold between sulci of pronotum; a deep transverse depression in front of posterior sulcus preceded by two small tubercles situated symmetrically on each side of median carina. Anterior margin of pronotal disc convex, slightly projecting, almost straight in centre or slightly emarginated (Fig. 6A); hind margin obtuse-angular (holotype), or rectangular and apex broadly rounded to subangular; median carina well developed reaching to median prozonal sulcus (highly

variable), faintly developed between median prozonal sulcus and posterior sulcus, in metazona complete and moderately elevated, thickened in anterior third, slightly attenuated near anterior and posterior margin of metazona; prozona crossed by three transverse sulci (Fig. 6A); anterior (submarginal) sulcus not crossing median carina, broad, little incised and sinuous, almost reaching lower margins of paranota; median prozonal sulcus short and sinuous, deeply cutting into median carina but hardly reaching lateral carinae; third prozonal sulcus deep, broadened abruptly in mid of paranota, extending ventrally almost to lower margins of paranota; posterior sulcus broadly and deeply cutting median carina far ahead of middle of pronotum, ventrally reaching to about mid of paranota; metazona 1.95–2.12 times longer than prozona (holotype: 2.04). Paranota 1.3–1.4 times higher than long; anterior margin slightly convex, lower margin thickened, particularly in distal half, always strongly inclined, trajectory variable (almost straight in the holotype, slightly concave or sinuous in paratypes), ventral third of posterior margin broadly rounded or subangular, straight or slightly curved in the rest, lower anterior angle obtuse-angular to rounded, lower posterior angle straight or rounded and moderately projecting, rarely forming a denticle (Fig. 6B).

Sternum: Sternal plate slightly wider than long, orange, rose, yellowish or whitish; mesosternum with coarse and dense brownish dots; mesosternal interspace 1.32–1.57 times wider than long (holotype: 1.37); metasternal interspace 1.88–2.30 times wider than long (holotype: 2.11), both interspaces clearly defined by deep sulci, which separate the meso- and metasternal lobes (Fig. 6C).

Legs: Hind femora 7.6–8.7 mm long (holotype: 7.6 mm), moderately robust to slender, 3.57–4.14 times longer than broad (holotype: 3.57); external side of hind femur ivory whitish with one complete pre-apical band situated at the same position as second tegminal band (Fig. 5A); brownish colour of band particularly well developed at the carinae and carinulae; a second less developed and incomplete band near mid of hind femur (in some specimens hardly visible); inner side of hind femur yellowish or pale brown, with three transverse dark bands, not surpassing lower carinula; first band basally, diffuse and little contrasting; second band slightly before the mid, brownish, always well developed and clearly separated from third one; third band pre-apical, blackish, stronger contrasting than other bands; apex paler than rest of leg, whitish to yellowish. External and upper internal genicular lobes of hind knee whitish, pale brownish or more or less mottled, lower internal genicular lobe black. Hind tibiae with 7–9 (8/8 in holotype) external spines and 10–12 internal spines (11/11 in holotype), spines apically blackish or brownish and basally whitish, yellowish or (most frequently) white-bluish; inner side of tibial condyle black, first quarter of hind tibiae white-yellowish, except for proximal part, which is black; second quarter brownish-bluish, brownish-purple, or purple; third quarter white-yellowish or white-bluish; apical quarter brownish, brownish-purple, or greenish. External side of tibiae basally blackish (except for condyle, which is bicoloured), distally whitish, coloration similar to internal part, but less contrasting; spurs basally yellowish, apically brown-blackish, apical pair longer than pre-apical pair, and internal pair longer than external pair. Inner apical spur slightly surpassing half of mid tarsal segment, about twice as long as basal width of tibia. Arolium of hind tarsi elongated oval, approximately three times longer than wide, as long or slightly longer than half of claw.

Wings: Tegmen 5.5–6.1 times longer than wide (holotype: 5.5), strongly surpassing hind knees (5.0–6.3 mm, holotype: 5.6 mm), costal margin convex in the basal quarter (Fig. 5A). Basic colour opalescent white, apical quarter scarcely pigmented; basal third brownish-yellowish or brownish-red, densely reticulated and mottled; two complete brown-blackish

transverse bands, sometimes with a third incomplete one (Fig. 5A); first band at beginning of second quarter, with continuous margins; second band situated midway, usually with continuous margins, sometimes deeply incised, but without isolated speckles; third band apically, composed of numerous isolated speckles, varying in size and number (6–10), in some specimens fused to form a third band (with discontinuous margins). Anterior margin convex in basal quarter; subcosta running parallel to radius, slightly separated but very close until end of medial area, diverging from there gradually to apex of tegmen; anterior part of radius running parallel to media, merging almost with media in proximal half of medial area, clearly separated and well developed distally, strongly diverging to apex of tegmen; 11–16 transverse veinlets (holotype: 14) between radius and media between external margin of first transverse band and apex of medial area, transverse veinlets strongly projecting above level of intercalary vein, laterally compressed and moderately distant from each other (mean interval 0.19–0.31 mm, holotype: 0.21 mm); radial sector with two ramifications (in one paratype only one), second branch usually sub-apical; media strongly attenuated and situated below level of radius to mid of medial area; intercalary vein not serrated, almost straight to moderately sinuous, continuous and only distally broken, apically nearly reaching apex of medial area and closer to media than to cubitus. Hind wings 1.6–1.9 times longer than wide (holotype: 1.7); wing disc basally sky blue, apically hyaline; central wing band brown-blackish, strongly contrasting, with well-defined margins (Fig. 5A), continuous from costal margin to V10–V12 (V11 in holotype).

Abdomen: Coloration dorsally brownish or brownish-yellow, except last sternites, which are yellowish; ventrally yellow to orange (in one, possibly immature, specimen beige). Subgenital plate acutely conical, apex blunt, not attaining level of epiproct. Cerci robust, 1.6–2.0 times longer than wide (holotype: 1.9), almost regularly conical, apex broadly rounded, sometimes slightly thickened in basal third (Figs 6D, 9B). Supra-anal plate pentagonal (Figs 6F, 8B, B'), ash-grey, with dark (bluish or brownish-purple) carinae; 1.01–1.11 times longer than wide (holotype: 1.07); carinae variable; lateral and internal basal carinae strongly projecting (sometimes laminar); basal and apical lobes laterally strongly expanded and margins slightly up-curved, both with posterior angle projecting, particularly first, which is triangular and about twice as long as wide; transverse carina weak, sometimes indistinct; carina of basal interlobular space forming a 'V', 'Y', or 'T', varying from strongly developed (in holotype) to nearly invisible, but always with

apical nodular process projecting above transverse carinae (Figs 6F, 8B, B'); internal apical carina variable: 'U'-shaped (as in holotype), 'Y'-shaped with very short central arm, reduced to two small curved carinae, which are converging but not apically linked, or presented as three conspicuous nodules arranged at the apex and in the centre of each arm (Figs 6F, 8B, N'); apical interlobular space slightly concave, in some cases with one or two additional denticles near centre (Figs 6F, 8B, B'); apex basally moderately widened, with margins obtuse-angular or straight and apically widely rounded or subangular.

Genitalia: Epiphallus nearly twice as wide as long (Fig. 10B); ancorae corniform, strongly separated and slightly diverging, in holotype distance between apices 0.6 mm; bridge of medium length and width, slightly arched; space between lateral plates trapezoidal; lateral plates with straight or slightly convex external margins; posterior projections oblique and denticular, anterior projections moderately thickened, angular; lophi small, bipartite, internal part transverse, external part oblique, both apices projecting (particularly external part).

Description of female

Habitus similar to male, but larger and stouter (Fig. 5B, D); total length from fastigium of vertex to end of tegmina 24.6–27.9 mm, to end of hind knee 18.4–20.6 mm.

Furthermore, the female differs from the male in the following characters:

Antennae proportionally shorter (0.7× length of hind femur, 1.1–1.2× combined length of head and pronotum); lateral carinae of vertex less developed, median carina nearly invisible; vertex width and minimum interocular distance proportionally greater, ratio between eye length and these two parameters 1.83–2.06 and 1.79–2.01, respectively. Subocular furrow as long as eye (ratio: 0.98–1.06).

Median carina of prozona less developed, always present, but little elevated; metasternal interspace proportionally wider, ratio width/length 2.32–2.67; as wide or slightly less wide than mesosternal interspace, ratio wMs/wMt 0.97–1.08.

Median band of hind femur incomplete or complete.

Transverse veinlets between radius and media similar to male, thickened, numerous (11–18), interval 0.19–0.27 mm; intercalary vein nearly straight to slightly sinuous, course regular, only distally broken and almost reaching apex of medial area.

Coloration generally less contrasting, particularly tegmina, posterior tibiae and ventral part of abdomen, which is brownish.

Hind margin of subgenital plate bilobate and with a deep sub-triangular notch with acute or straight angle (Figs 6G, 9N, N').

Cerci short, 1.2–1.7 times longer than wide, robust and conical (Fig. 6E, 9H).

Ovipositor relatively short (Fig. 6G), valves basally smooth with just some small scattered callosities, apically robust, 1.5–1.6 times longer than wide; transverse carina of basal part little developed.

Etymology

The epithet refers to the characteristic apical nodular process of the basal interlobular space of the male supra-anal plate.

DIFFERENTIAL DIAGNOSIS

Within the genus *Sphingonotus*, *S. (N.) nodulosus* sp. nov. belongs to the group of species with thickened cross-veinlets between radius and media (subgenus *Neosphingonotus*). On the Iberian Peninsula three other species show this stridulatory mechanism, namely *S. azurescens*, *S. morini* and *S. almeriense* sp. nov., while all other species have the typical Oedipodinae stridulatory mechanism, the serrate intercalary vein, including *S. imitans* comb. rev. which branched off as a sister species to *S. nodulosus* in the molecular analysis (Fig. 1). The coloration of the wing disc of *S. nodulosus* sp. nov. is basally bluish with a conspicuous dark band in the centre and is apically hyaline (Fig. 5A, B), differing from nearly all taxa in the subgenus *Sphingonotus*: *S. caeruleans* has bluish wings without a band, *S. imitans* comb. rev., *S. lusitanicus* comb. rev., and *S. rubescens* have hyaline or slightly bluish wings without a band, and *S. octofasciatus* has red wings with two dark bands. Within the subgenus *Neosphingonotus*, *S. nodulosus* sp. nov. differs clearly from other Iberian and North African species with a dark wing band [*S. (N.) canariensis*, *S. (N.) finotianus*, *S. (N.) tricinctus*, *S. (N.) paradoxus*, *S. (N.) pachecoi*] in the morphology of the external genitalia, particularly the male supra-anal plate and cerci and the female subgenital plate.

S. nodulosus sp. nov. is the only species, in which the male supra-anal plate has a carina in the basal interlobular space, which always ends in a conspicuous nodular process (Figs 6F, 8B, B'). Furthermore, the male supra-anal plate is slightly longer than wide (1.01–1.10 times), differing from *S. azurescens*, *S. morini*, *S. canariensis*, *S. finotianus*, and *S. pachecoi* (Fig. 8), in which it is wider than long (1.1–1.7 times) and from *S. almeriense* sp. nov. and *S. imitans* comb. rev., in which it is much longer than wide (1.3 times). Only in *S. paradoxus* is the proportion likely to be similar, although in this case the supra-anal plate is more angular and projected in the distal half,

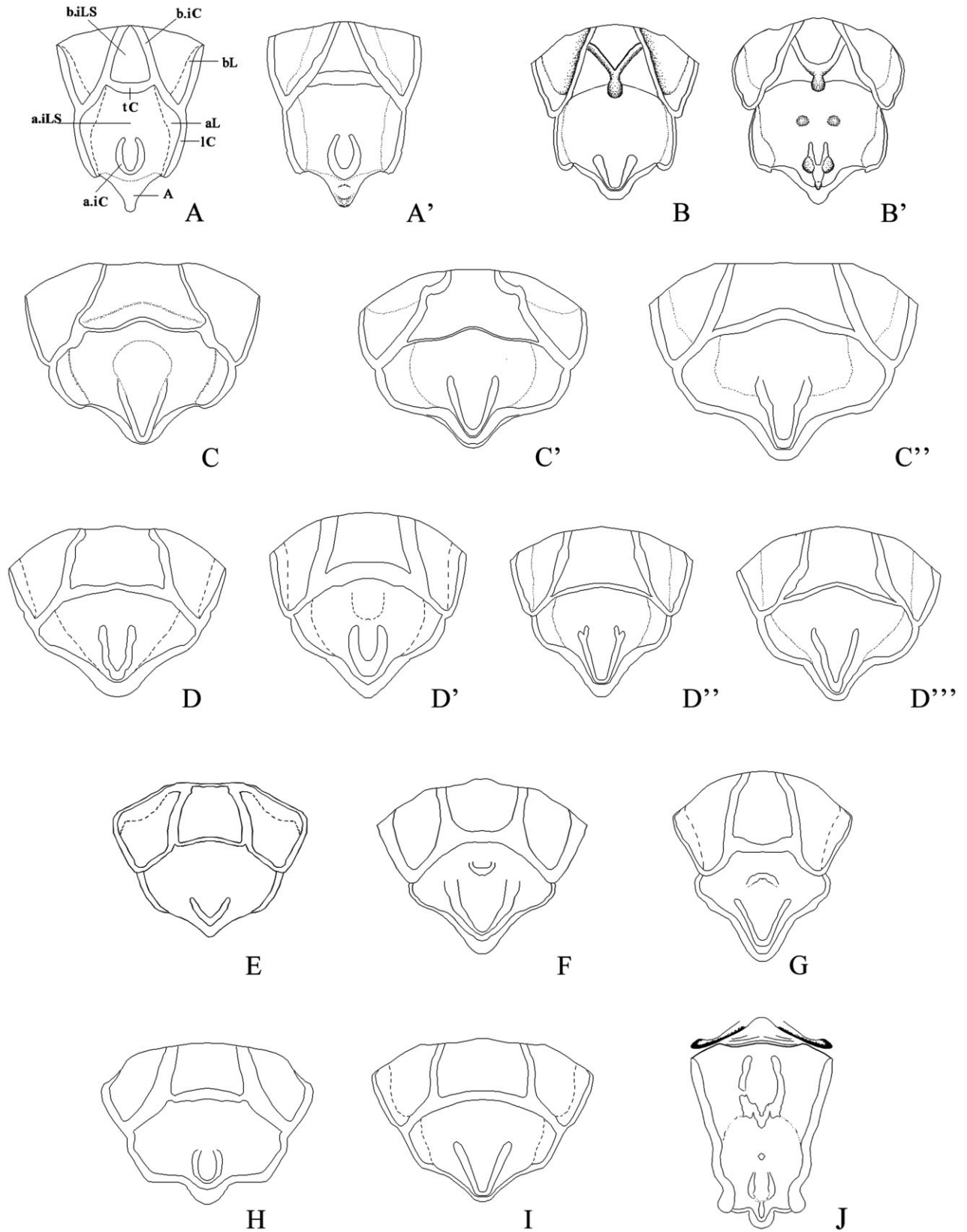


Figure 8. Male supra-anal plate in dorsal view of Iberian and North African species: A, *Sphingonotus (N.) almeriense* sp. nov. (holotype); A', *Sphingonotus (N.) almeriense* sp. nov. (paratype); B, *S. (N.) nodulosus* sp. nov. (holotype); B', *S. (N.) nodulosus* sp. nov. (Portugal, Leiria); C, *S. (N.) azurescens* (Spain, Huelva); C', *S. (N.) azurescens* (Spain, Málaga); C'', *S. (N.) azurescens* (Portugal, Bragança); D, *S. (N.) morini* (paratype, Spain, Zaragoza); D', *S. (N.) morini* (Spain, Almería); D'', *S. (N.) morini* (Spain, Almería); D''', *S. (N.) morini* (Spain, Lleida); E, *S. (N.) pachecoi* (Spain, Canary Islands, Lanzarote); F, *S. (N.) canariensis* (Mali); G, *S. (N.) paradoxus* (Arabia); H, *S. (N.) finotianus* (Morocco); I, *S. (N.) tricinctus* (Tunisia); J, *S. (S.) imitans* comb. rev. (Spain, Huelva). Terminology: tC, transverse carina; lC lateral carina; b.iC, basal-internal carina; a.iC, apical-internal carina; bL, basal lobe; a.iLS, apical interlobular space; b.iLS, basal interlobular space; aL, apical lobe; A, apex.

and no carinae exist in the basal interlobular space (Fig. 8G). *Sphingonotus nodulosus* sp. nov. is also the only species in which the cerci are almost regularly conical (Figs 6D, 9B), while in the other species they are cylindrical (Fig. 9) or abruptly narrowed in the middle (*S. almeriense* sp. nov., Fig. 9A). In the females, the posterior margin of the subgenital plate is deeply and narrowly excised (Figs 6G, 9N, N'), which is only found in *S. almeriense* sp. nov. However, in the latter species the excision is flanked by two conspicuous extensions (which are sometimes nearly dentiform; Fig. 9M), while in *S. nodulosus* sp. nov. it is bilobate (Fig. 9N, N').

Sphingonotus nodulosus sp. nov. is conspicuously smaller than *S. azurescens*, *S. finotianus*, *S. paradoxus*, and *S. tricinctus*. The antennae are slightly widened in the apical third (more pronounced in males; Fig. 6A) and proportionally shorter than in *S. azurescens* and *S. morini* (particularly in males). The dark wing band is strongly contrasting brown-blackish, not interrupted and extends at least until V10 (Fig. 5A, B). In *S. finotianus* the wing band is only indicated by a dark infumation of the vannal veins. In *S. almeriense* sp. nov. the wing band is interrupted, less contrasting, and usually ends before V9. In *S. pachecoi* the apex is slightly infumated. Among the Iberian *Neosphingonotus* species, *S. nodulosus* sp. nov. differs from *S. azurescens* and *S. morini* by its longer area of transverse veinlets between radius and media, which are also more pronounced. In both sexes the transverse veinlets are closer together than in *S. almeriense* sp. nov. The hind tibiae have two purplish to brownish-purple rings, while they are generally bluish, greenish, or rarely brownish in other Iberian species. In the female, the metasternal interspace is proportionally wide (2.3–2.7 times wider than long), while it is < 2.3 times wider than long in other Iberian species.

Compared with *S. almeriense* sp. nov., the apical valves of the female ovipositor are more robust in *S. nodulosus* sp. nov. (< 1.6 times longer than wide; Figs 4G, 6G), the subocular furrow is longer (ratio eye length/length of subocular furrow: 0.97–1.06; *S. alm-*

eriense sp. nov.: 1.08–1.24), and the male epiphallus has a longer and more slender bridge; the ancorae are slightly diverging and much stronger separated (Fig. 10A, B).

DISTRIBUTION, ECOLOGY AND BIONOMICS

The species is currently known from three localities in the southern half of the Iberian Peninsula: Lagoa de Óbidos (Leiria, Portugal), Puerto de Santa María (Cádiz, Spain), and Mora (Toledo, Spain; Fig. 12E), where it occurs in the central dunes and sandy beaches and other sandy habitats. It is probably strictly sabulicolous. At the type locality (Lagoa de Óbidos) *S. nodulosus* sp. nov. co-occurs with *S. azurescens*, but at much lower density (P. Lemos, pers. comm.).

THE STATUS OF THE GENERA GRANADA KOÇAK & KEMAL, 2008 AND SPHINGODERUS BEI-BIENKO, 1950

The genus *Granada* was monotypic, with *Sphingonotus imitans* Brunner von Wattenwyl, 1882 being the type species. Harz (1975) erected the genus *Jacobsiella* Harz, 1975 for *S. imitans* on the basis of its body size, the shape of the intercalary vein, the supra-anal plate, cerci, and the ratio between the length of the eyes and vertex width. Since the genus name *Jacobsiella* was preoccupied by a Dipteran genus, the new name *Granada* Koçak & Kemal, 2008 was given (Eades *et al.*, 2013). In our phylogeny *S. imitans* is clearly an ingroup taxon, i.e. a *Sphingonotus* species. As the generic traits provided by Harz (1975) are highly variable within the genus *Sphingonotus*, the original generic affiliation is herewith restored. *Granada* Koçak & Kemal, 2008 and *Jacobsiella* Harz, 1975 become synonyms of *Sphingonotus sensu stricto*.

The genus *Sphingoderus* currently comprises two species: *Sphingoderus carinatus* and *Sphingoderus angustus* Descamps, 1967, with the former assigned as type species. This taxon was given subgeneric rank within *Sphingonotus* by some authors (e.g. Harz,

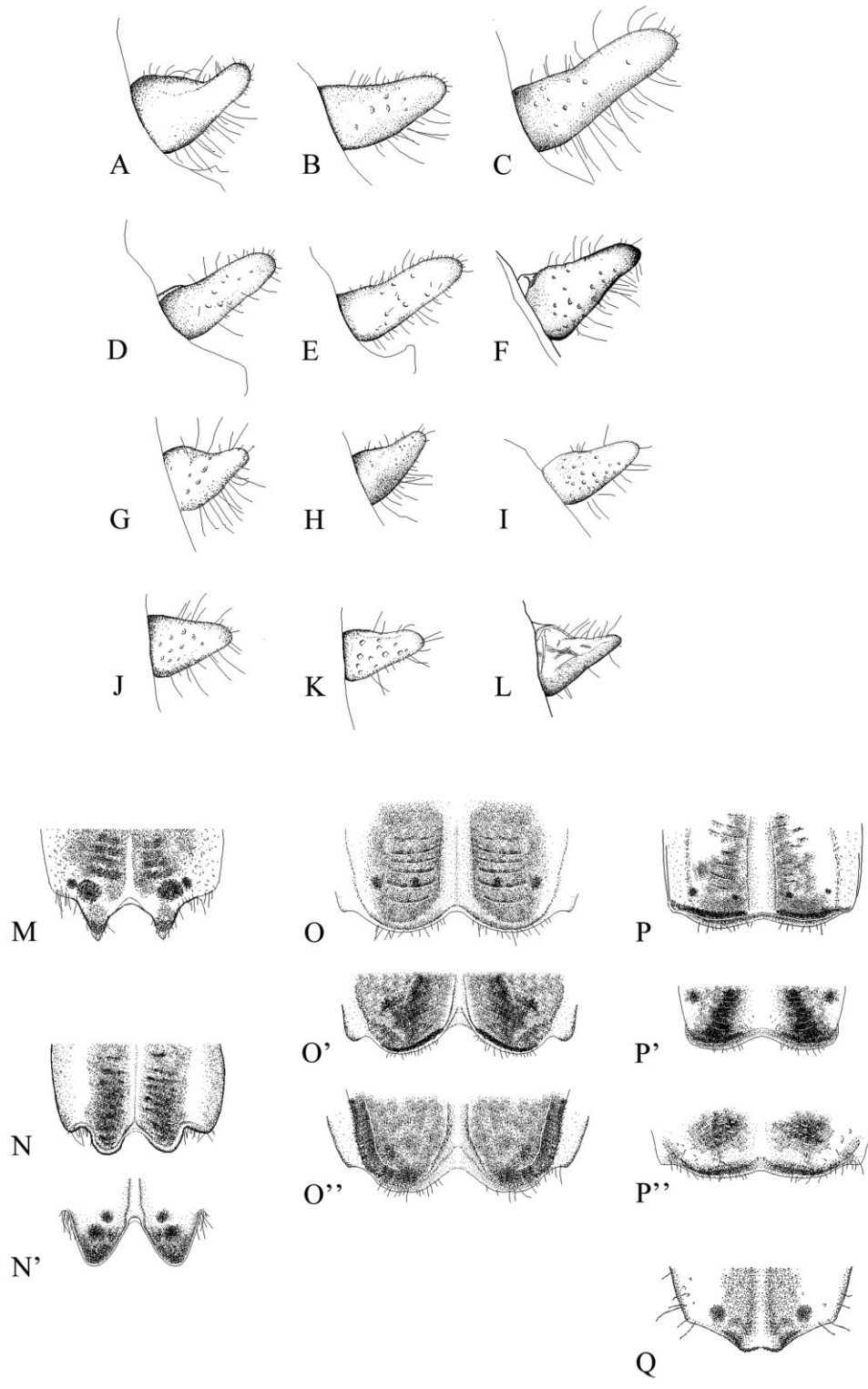


Figure 9. Male (A–F) and female cerci (G–L) in lateral view: A, G, *Sphingonotus (N.) almeriense* sp. nov. (male holotype and female paratype); B, H, *S. (N.) nodulosus* sp. nov. (male holotype and female paratype); C, I, *S. (N.) azurescens* (male from Spain, Málaga; female from Spain, Huelva); D, J, *S. (N.) morini* (male from Spain, Zaragoza; female from Spain, Huesca); E, K, *S. (N.) morini* (male from Spain, Almería; female from Spain, Granada); F, L, *S. (S.) imitans* comb. rev. (male and female from Spain, Huelva). Apical end of female abdomen (subgenital plate) in ventral view (M–Q): M, *S. (N.) almeriense* sp. nov. (paratype); N, N', *S. (N.) nodulosus* sp. nov. (paratypes); O, *S. (N.) azurescens* (Spain, Málaga); O', *S. (N.) azurescens* (Spain, Huelva); O'', *S. (N.) azurescens* (Spain, Cáceres); P, *S. (N.) morini* (paratype, Spain, Huesca); P', *S. (N.) morini* (Spain, Almería); P'', *S. (N.) morini* (Spain, Granada); Q, *S. (S.) imitans* comb. rev. (Spain, Huelva).

1975). In contrast to *Granada* our phylogenetic analysis strongly supports the genus rank for *Sphingoderus*. Additionally, *S. octofasciatus* branched off as a sister clade to *Sphingoderus*, suggesting that this clade may also deserve genus rank. However, a broader sampling of related outgroups and ancient *Sphingonotus* species is needed before taxonomic changes are made (see above).

THE STATUS OF *SPHINGONOTUS LUSITANICUS* EBNER, 1941 COMB. REV.

Sphingonotus lusitanicus comb. rev. has long been regarded a subspecies of *Sphingonotus candidus* Costa, 1888. Another former subspecies of *Sphingonotus candidus*, *S. personatus* Zanon, 1926, has meanwhile been given species rank (La Greca, 1994), a status which has widely been accepted (e.g. Willemse & Willemse, 2008). We here give *S. lusitanicus* comb. rev. species rank. In the phylogeny it branches off as a sister species to *S. lluciapomaresi*. Morphologically, Harz (1975) already stated that *S. candidus* and *S. lusitanicus* comb. rev. differ in their mesosternal interspaces (which is 2× wider than long in *S. candidus*, but only 1.25× wider than long in *S. lusitanicus* comb. rev.). In addition, *S. lusitanicus* comb. rev. is larger than *S. candidus* (total length from vertex to tip of tegmen: ♂ > 25 mm, ♀ > 32 mm). Furthermore, the intercalary vein is vaguely serrated in *S. lusitanicus* comb. rev. (while the serration is distinct in *S. candidus*), the tegmen have no transverse band (while one or two bands can be present in *S. candidus*), and the number of secondary branches of the radial sector is higher: three in males (rarely two), three to four in females, while usually only two branches exist in *S. candidus* in both sexes. The coloration of the hind tibiae is much more homogenous in *S. lusitanicus* comb. rev. (whitish or yellowish, only slightly darkened apically and without any contrasting bands), while in *S. candidus* the hind tibiae are brownish basally with a contrasting grey-bluish apical part. There are also differences in the external genitalia. In *S. lusitanicus* comb. rev. the inner carinae of the male supra-anal plate are basally

larger and protruding, the lateral lobes are laterally also protruding and upwards curved, the lateral margins are strongly sinuous and angular at the point of union between basal and apical lobes. In *S. candidus*, the inner carina is basally weak and the lobes are only moderately expanded with slightly sinuous lateral margins.

THE STATUS OF *SPHINGONOTUS CALLOSUS* (FIEBER, 1853)

The original description of *Oedipoda callosa* by Fieber (1853) is based upon the following characters: colour grey or reddish-yellow, head whitish with black dots; pronotum rugose with elevated transverse bulge, 'process' (probably the pronotum is meant) with forked white callosities and granules, hind margin excised; inner side of hind femora with broad black basal band; hind tibia pale greenish, basis, mid and apex brownish. Unfortunately, the type locality is very imprecise ('Spain'). Brunner von Wattenwyl (1882) mentions that two different species have been recorded under this name: the 'true *S. callosus*' from Spain and one which occurs from North Africa to Central Asia. Mistshenko (1936) followed the interpretation of Brunner von Wattenwyl (1882) and described a new species (*S. eurasius*) from the eastern part of the range, while he synonymized *S. callosus* with *S. azurescens*. The synonymy has broadly been accepted (but see Uvarov, 1948) and *S. callosus* has no longer been cited for the Iberian Peninsula (e.g. Harz, 1975). However, recently the species re-appeared in a key to the Egyptian *Sphingonotus* species (Abdel-Dayem *et al.*, 2005). The confusing status of this species is exemplified by the database of Eades *et al.* (2013), where it occurs twice (once as a synonym of *S. azurescens* and once as a valid species).

To our knowledge the type material of *S. callosus* is lost (Eades *et al.*, 2013). However, Brunner von Wattenwyl (1882) mentioned that material of *S. callosus* collected by Fieber in Spain was handed to him. As the Brunner von Wattenwyl collection was stored in the Natural History Museum Vienna, we started an enquiry at this museum, which was negative (H.

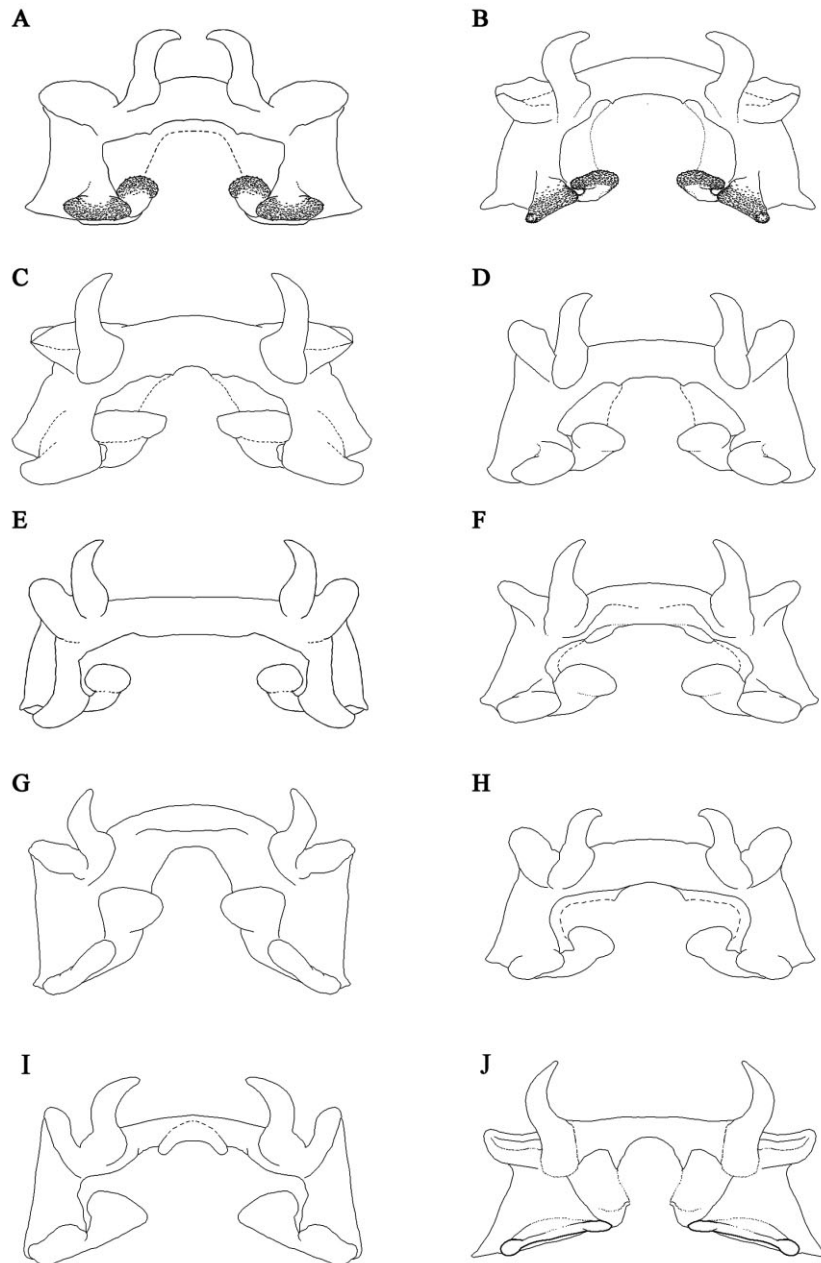


Figure 10. Epiphallus in dorsal view of: A, *Sphingonotus (N.) almeriense* sp. nov. (holotype); B, *S. (N.) nodulosus* sp. nov. (holotype); C, *S. (N.) azurescens* (topotype, Spain, Málaga); D, *S. (N.) morini* (paratype, Spain, Zaragoza); E, *S. (N.) pachecoi* (Spain, Canary Islands, Lanzarote); F, *S. (N.) tricinctus* (Tunisia); G, *S. (N.) paradoxus* (Tunisia); H, *S. (N.) canariensis* (Cap Verde); I, *S. (N.) finotianus* (Morocco); J, *S. (S.) imitans* comb. rev. (Spain, Huelva).

Bruckner, pers. comm.). As it is impossible to examine the type material, only the traits mentioned by Fieber can be used to prove its taxonomic identity. Among the Iberian species of *Sphingonotus*, several species match the description (*S. azurescens*, *S. lluciapomaresi*, *S. morini*, *S. gypsicola*, *S. almeriense* sp. nov., *S. nodulosus* sp. nov.). The shape of the pronotum can vary substantially within and among species. Further-

more, the colour pattern described by Fieber does not match in detail to any of these species, although it might be partly compatible with *S. azurescens*, *S. morini*, or *S. gypsicola*. However, colour polymorphism is strong in most Oedipodinae and it might vary depending on the storage and treatment with chemicals. Therefore, *S. callosus* should be treated as *nomen dubium* rather than as a synonym of *S. azurescens*.

KEY TO THE IBERIAN *SPHINGONOTUS* SPECIES

1. Intercalary vein of tegmina in males serrate (Fig. 7E), projecting above radius and media, in females sometimes less serrate or smooth; radial area at the same level as medial area, without cross veinlets between radius and media.....subgenus *Sphingonotus* **2**
 - Intercalary vein of tegmina smooth (very rarely with serration); radius and media little separated with thickened cross veinlets between them (Fig. 7A–D), which are less developed in females, projecting above the intercalary vein.....subgenus *Neosphingonotus* **8**
(note that *S. S. savignyi* may possess both types of stridulatory mechanisms, in single cases, *S. S. azurescens* and *S. S. morini* could also possess a vestigial serration of the intercalary vein)
2. Hind wings bluish or hyaline and with or without one dark band.....**3**
 - Hind wings red with two dark bands, one in the mid and one at the apex (Depression of Guadix and Baza)....
.....*S. octofasciatus*
3. Hind wings bluish or hyaline without any dark trace or band, sometimes with black vannal veins.....**4**
 - Hind wings bluish with dark transverse band.....**7**
4. Internal apical spur of hind tibiae as long or slightly shorter than first tarsal segment; inner side of hind femora pale (yellowish to light brownish), with or without dark fascia; tegmen finely dotted without transverse bands; hind femora slender, often 4× longer than wide (only found in sandy coastal habitats).....**5**
 - Internal apical spur of hind tibiae much shorter than first tarsal segment (*c.* half as long); inner side of hind femora dark brown with one or two pale, more or less complete transverse fasciae; tegmen crossed by one or two dark bands (the basal one more contrasting); hind femora more robust, < 4× longer than wide.....**6**
5. Large species, total length (V-T) in males > 25 mm, in females > 32 mm; tegmen long with apex reaching almost end of hind tibiae; fore and mid femora 7–8× longer than wide; male supra-anal plate pentagonal, wider than long; male cerci cylindrical, > 2 times longer than wide, conical in females and > 1.5 times longer than wide (coastal dunes and beaches in south-west Iberia: Huelva, Faro).....***S. lusitanicus* comb. rev.**
 - Small species, total length (V-T) in males < 23 mm, in females < 28 mm; tegmen short with apex ending far ahead of the end of the hind tibiae; fore and mid femora 9–10× longer than wide; male supra-anal plate rectangular, longer than wide (Fig. 8J); cerci pear-shaped, in males < 2 times longer than wide (Fig. 9F); in females 1.5 times longer than wide (Fig. 9L) (sandy coastal habitats in south-west Iberia: Granada, Cádiz, Huelva, Faro, Setubal, Leiria).....***S. imitans* comb. rev.**
6. Hind wings hyaline; transverse bands of tegmen weakly defined with discontinuous margins (particularly the 2nd and 3rd band), usually built by a variable number of speckles; intercalary vein variable but never straight, often sinuous with apical part close to media; male supra-anal plate brownish to yellowish-brown, broadly triangular with medial lobes slightly widened and gradually narrowing towards the apex (Mediterranean part of the Iberian Peninsula).....*S. rubescens*
 - Hind wings bluish (sometimes only weakly in the basal part); transverse bands of tegmen distinct and continuous (particularly the 1st and 2nd band); intercalary vein variable but never markedly sinuous, usually straight with apical part separated from the media; male supra-anal plate blue or brown-bluish, pentagonal with apical lobes broadened and apically abruptly narrowed (nearly whole Iberian Peninsula).....
.....*S. caeruleans*
7. Head and vertex proportionally broad compared with length of eye; ratio between the length of the eye (LE) and minimum inter-ocular distance (iO) ≤ 2 in males and ≤ 1.7 in females; intercalary vein in males coarsely serrated, number of teeth (counted at the end of the precostal lobe) per 5% of tegmen length < 40; external area of hind femora with two little contrasting brownish, transverse bands; margins and carinae of supra-anal plate yellowish, sometimes brownish, never blue; ventral valves of ovipositor robust, length ≤ 1.5× its maximal basal width (gypsum soils of eastern Iberia).....*S. gypsicola*
 - Head and vertex proportionally narrow compared with length of eye; index LE/iO ≥ 2 in males and > 1.7 in females; intercalary vein in males densely serrated, number of teeth per 5% of tegmen length ≥ 40; external area of hind femora with only one strongly contrasting brown-blackish or blackish transverse band, coinciding with the second transverse band of the tegmen; margins and carinae of supra-anal plate blue to pale-bluish; ventral valves of ovipositor narrow, length ≥ 1.5× its maximal basal width (silicious soils of the Mediterranean Region of Iberian Peninsula).....*S. lluciapomaresi*
8. Antenna short, in males ≤ 1.3× longer than head and pronotum together (Figs. 4A, 6A), in females ≤ 1.2×; arolium of hind tarsi elongated, *c.* 3× longer than wide and *c.* as long as or even slightly longer than half of the first claw; cross veinlets between radius and media conspicuous (particularly in distal half), projecting above the intercalary vein (Fig. 7A), which is always plain; male supra-anal plate longer than wide (Fig. 8A–B') (1.01–1.33); cerci in both sexes basally strongly thickened or regularly conical (Fig. 9A, B, G, H), in males < 2.1× longer than wide; hind margin of female subgenital plate deeply excised (Fig. 9M–N').....**9**

- Antenna long, in males > 1.3× longer than head and pronotum together, in females > 1.2×; arolium of hind tarsi rounded, *c.* 2× longer than wide and clearly shorter than half of the first claw; cross veinlets between radius and media less developed and only slightly projecting above or on the same level of the intercalary vein (Fig. 7D), which can be plain or vaguely serrated; male supra-anal plate wider than long (Fig. 8C–D''); cerci in males cylindrical and slender, > 2.1× longer than wide (Fig. 9C–E), in females conical (Fig. 9I–K); hind margin of female subgenital plate moderately concave or slightly excised (Fig. 9O–P'')..... 10
9. Male antennae filiform, apically not widened and only slightly longer than head and pronotum together (Fig. 4A) (< 1.2×); dark wing band brownish, little contrasting, interrupted between cubitus and vena dividens and with diffuse margins, reaching to V8–V10 in males and V7–V8 in females (Fig. 3A, B); cerci in both sexes basally thick and abruptly narrowing in the middle and apically cylindrical (Fig. 9A, G); male supra-anal plate much longer than wide (1.3×) with little developed carinae (Fig. 8A, A'); posterior margin of female subgenital plate excised with two denticles or elongated lobes (Fig. 9M) (Cabo de Gata, Almeria)..... ***S. almeriense sp. nov.***
- Male antennae slightly widened in distal third (in females only slightly), 1.2–1.3× longer than head and pronotum together (Fig. 6A); dark wing band brown-blackish, strongly contrasting, in both sexes uninterrupted and with distinct margins, reaching to V10–V12 (Fig. 5A, B); cerci in both sexes regularly conical (Fig. 9B, H); male supra-anal plate slightly longer than wide (max. 1.1×) with distinct carinae, basal interlobular space with a carina (generally forming a 'V') extending to an apical nodular process (Fig. 8B, B'); posterior margin of female subgenital plate widely bilobate and deeply excised (Fig. 9N, N') (southern part of Iberian Peninsula)..... ***S. nodulosus sp. nov.***
10. Body size usually large (males 24–31 mm, females 31–40 mm); head slender and higher, vertex narrow and face elongated compared with body length; ratio between length of subocular furrow and minimum inter-ocular distance usually > 1.6 (particularly in males); female tegmen usually slightly widened from precostal lobe to end of medial field (ratio width at apex of medial area/width at apex of precostal lobe: 1.00–1.08); dark fascia of hind wing in both sexes contrasting brownish-black, margins distinct, always continuous, and reaching at least to V12, often to V13–V14; cerci of both sexes long (Fig. 9C, I) (males: 1.01–1.34 mm; females: 0.60–0.82 mm); male supra-anal plate broad (1.2–1.7× wider than long), shape pentagonal, lateral margins sinuous and apically abruptly narrowed (Fig. 8C–C''); ratio between maximum width of supra-anal plate and minimum inter-ocular distance > 1.7; hind margin of female subgenital plate bilobate, with a narrow and moderately deep incision (Fig. 9O–O'') (western half of Iberia)..... *S. azurescens*
- Body size smaller (males 19–26 mm, females 26–33 mm); head more compact, vertex wider and face less elongated compared with body length, ratio between length of subocular furrow and minimum inter-ocular distance usually < 1.6 (particularly in males); female tegmen generally narrowed from the precostal lobe, only occasionally slightly widened near the apex of the medial field (ratio width at apex of medial area/width at apex of precostal lobe: 0.90–1.01); dark fascia of hind wing variable, often brownish with diffuse margin and more or less interrupted, in females much more constant, in some cases the band can be nearly completely reduced; cerci in both sexes shorter (Fig. 9D, E, J, K) (males: 0.75–1.05 mm; females: 0.42–0.62 mm); male supra-anal plate narrower (1.0–1.4× wider than long), near-triangular, lateral margins slightly sinuous and continuously narrowing towards apex (Fig. 8D–D''); ratio between maximum width of supra-anal plate and minimum inter-ocular distance < 1.7; hind margin of female subgenital plate concave with broad and flat incision (Fig. 9P–P'') (eastern half of Iberia)..... *S. morini*

DISCUSSION

In recent decades the use of DNA markers for species delimitation has become increasingly widely used (e.g. Hebert *et al.*, 2004; Smith *et al.*, 2006; Vieites *et al.*, 2009). However, the use of mtDNA is also known to be associated with problems caused by introgression and incomplete lineage sorting (e.g. Moore, 1995; Shaw, 2002; Funk & Omland, 2003; Maddison & Knowles, 2006; Toews & Brelsford, 2012). In our phylogenetic analysis, we found no clear resolution for some taxa. This is particularly true for the *S. caerulans*-group and the *S. azurescens*-group, both of which contain several morphologically or bioacoustically well-distinguished, but genetically poorly differentiated species (at least at the studied loci). Although our phylogeny does not support the species

level of all taxa, we retain their species status as this is supported by other characters (either morphology or bioacoustics). It is well known that prezygotic reproductive isolation often evolves before fixed genetic differences can accumulate and becomes reinforced in sympatry (Coyne & Orr, 1989). We interpret our results as two flocks of incipient species evolved during recent radiations, which have not yet accumulated enough substitutions to represent reciprocally monophyletic lineages. Although it is not possible to provide reliable divergence time estimates for these groups due to the lack of reliable calibration points (particularly fossils), the low p-distances (< 0.014) among the species in both groups suggest that they cannot be very old. Similar patterns of phenotypically or bioacoustically distinct and reproductively isolated species showing a lack of genetic differentiation have

been found in other recent grasshopper radiations (Mason, Butlin & Gacesa, 1995; Carstens & Knowles, 2007).

Several terminal branches of the phylogenetic tree were rather short (e.g. the p-distance between *S. caerulans atlas* and *S. rubescens* was only 0.006). Nevertheless, *S. rubescens* has a unique melodious song, which is not found in any other *Sphingonotus* species (Husemann & Hochkirch, 2007). Former records of *S. corsicus* from the Iberian Peninsula are probably erroneous and based upon confusion with *S. rubescens*. Both species have a sinuous intercalary vein, but the song presented by García *et al.* (1997) for *S. corsicus* from Spain clearly matches the song of *S. rubescens*. Meanwhile it is evident that *S. corsicus* does not occur on the Iberian peninsula (Default, 2003). This observation points out the need for the integration of bioacoustic, behavioural, and morphometric analyses to assess the status of these taxa conclusively. Although our study is quite comprehensive, some of our findings deserve more intense treatment in the future. For example, *S. caerulans* turned out to be polyphyletic with three mtDNA lineages. In particular, specimens from Central and northern Europe (including those from the type locality and the subspecies *S. c. cyanopterus*) are genetically clearly different from those from south-west Europe (France, Spain, and the Balears). While the former group seems to be related to *S. lluciapomaresi*, *S. lusitanicus* comb. rev., and *S. corsicus*, the latter group and specimens from Morocco (subspecies *S. c. atlas*) seem to be sister clades of *S. rubescens*. The branch lengths of these clades are quite similar to other taxa with species status. It is therefore plausible that these three lineages represent three different species, but on the other hand, the small genetic distances between these clades might also suggest that these taxa are not yet fully reproductively isolated. Furthermore, some of the phylogenetic relationships are only weakly supported (PP < 50). Hence, we conclude that it is premature to infer species status for any of these clades.

Another interesting result is that *S. gypsicola* is completely nested in the south-west European *S. caerulans* clade. There are four potential explanations for this result: (1) recent introgression, (2) incomplete lineage sorting, (3) too low resolution of the molecular markers, or (4) a combination of these phenomena. During a preliminary phylogenetic analysis, we also found that *S. gypsicola* became a distinct sister group to the Iberian *S. caerulans* when *S. c. atlas* was excluded. This suggests that homoplasy might affect the position of these clades, and more genes (particularly nuclear loci) need to be studied to unravel the true relationships. A similar problem concerns a clade comprising specimens of

S. morini, *S. azurescens*, *S. tricinctus*, *S. sublaevis*, and *S. pachecoi*, which have very low genetic distances (p-distance 0.001–0.004). Only *S. pachecoi* formed a monophylum in this group, while *S. tricinctus* was nested in a clade comprising also *S. azurescens* and *S. morini*. It is thus possible that speciation is not yet completed in all of these taxa. Furthermore, some specimens of *S. azurescens* and *S. morini* even branched together with *S. finotianus*, which is genetically and morphologically the most differentiated species in the *S. azurescens*-group. This pattern remained constant even after a second DNA extraction from the original material, supporting that it has not been caused by contamination. It is much more likely that introgression is the main reason for this pattern, particularly as *S. azurescens* seems to have similar courtship behaviour to *S. finotianus* (P. Edelaar, pers. comm.). In mate choice experiments, *S. finotianus* from Morocco and *S. cf. azurescens* from Morocco was the only species pair which showed no significant preference for conspecifics (A.H., unpubl. data).

Our data show that three *Sphingonotus* species from the Iberian Peninsula are coastal endemics (Figs 11, 12): *S. imitans* comb. rev. occurs along the southern and western coast, *S. lusitanicus* comb. rev. is found at the southern Atlantic coast, and *S. almeriense* sp. nov. occurs at the Cabo de Gata-Níjar. This suggests that the coastline of the Iberian Peninsula played an important role as a refuge for *Sphingonotus* species during periods of adverse climatic conditions. Interestingly, the two coastal species with overlapping ranges (*S. imitans* comb. rev. and *S. lusitanicus* comb. rev.) seem to be ecologically separated. While *S. lusitanicus* comb. rev. inhabits beaches and dunes, *S. imitans* comb. rev. is found behind these dunes (edges of pine forests etc.). A surprising result of our phylogenetic reconstruction was that *S. lusitanicus* comb. rev. belongs to the *S. caerulans*-group and seems to be closely related to *S. lluciapomaresi*. Morphologically, this species is close to *S. candidus* and *S. personatus*. The rather similar morphology of these three taxa (which have formerly been regarded as subspecies of *S. candidus*) and also *S. imitans* comb. rev. might be a result of convergence; all three species occur in dunes and display specific morphological adaptations (long mid legs and spurs, flattened body). Another explanation for the conflicting morphology and molecular phylogeny might be found in a past introgression event of mtDNA into the genome of *S. lusitanicus* comb. rev. and/or *S. imitans* comb. rev.

Another surprising result of the molecular analysis is the close phylogenetic relationship of *S. imitans* comb. rev., *S. nodulosus* sp. nov., and *S. almeriense* sp. nov. The latter two species possess well-developed thickened cross veinlets between radius and media,

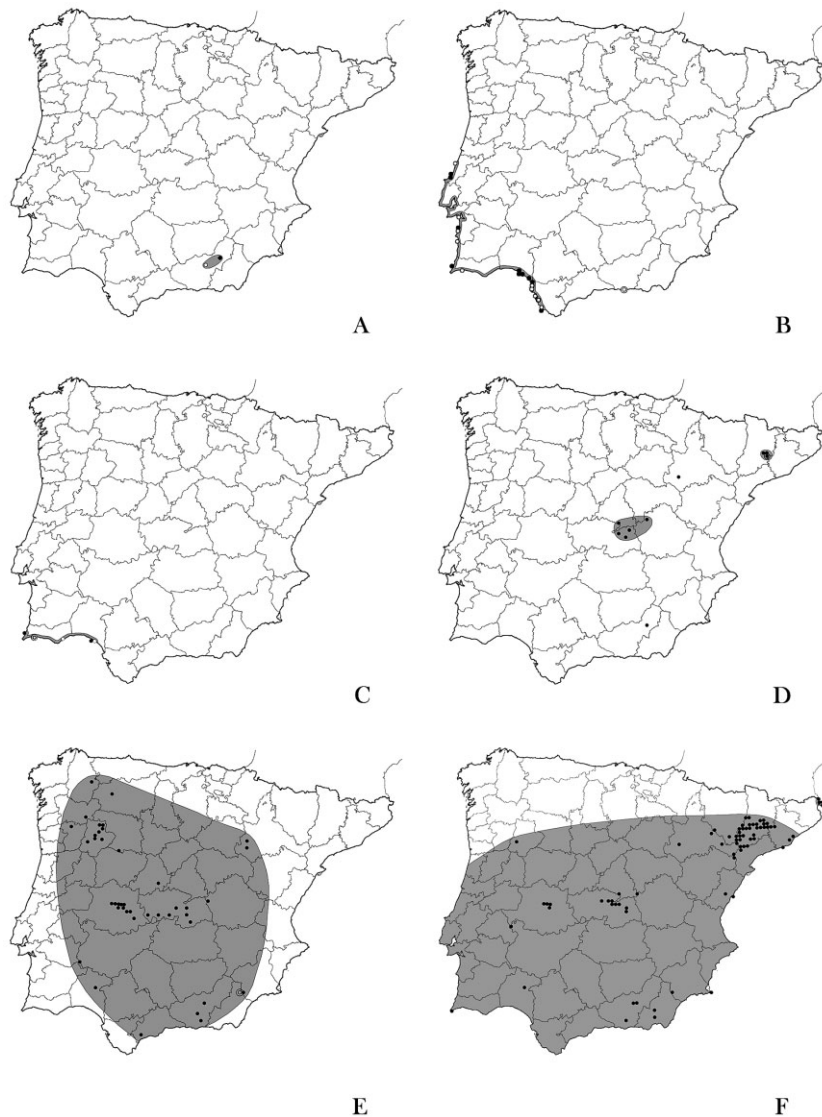


Figure 11. Maps of the known records of: A, *Sphingonotus* (*S.*) *octofascitatus*; B, *S. (S.) imitans* **comb. rev.**; C, *S. (S.) lusitanicus* **comb. rev.**; D, *S. (S.) gypsicola*; E, *S. (S.) lluciapomaresi*; F, *S. (S.) rubescens*. Filled circles: material studied by the authors; open circles: records from the literature (only unproblematic species considered); circled records: type localities.

which is very likely to be a synapomorphy of the genus *Neosphingonotus*, whereas *S. imitans* **comb. rev.** has the plesiomorphic character state (serrated intercalary vein). Two hypotheses might explain this pattern: (1) secondary loss of the apomorphic character state (the intercalary vein is also present in several *Neosphingonotus* species and sometimes slightly serrated, so that its original function might easily re-evolve); and (2) a past introgression event with the ancestral species of *S. nodulosus* sp. nov. and *S. almeriense* sp. nov. The overlap of the geographical ranges of these three taxa supports the latter hypothesis

(Toews & Brelsford, 2012). In conclusion, our results show that the evolutionary history of the genus *Sphingonotus* was probably very complex, full of morphological and bioacoustic innovations and that the systematics of this species-rich genus is still not fully resolved. The genus represents a valuable model system for studying rapid evolutionary diversification.

A vast amount of literature is meanwhile available supporting the hypothesis that the Iberian Peninsula did not only serve as a refuge area for temperate taxa (Hewitt, 1999), but also that multiple 'refugia within refugia' may occur (Gómez & Lunt, 2006). Similar to

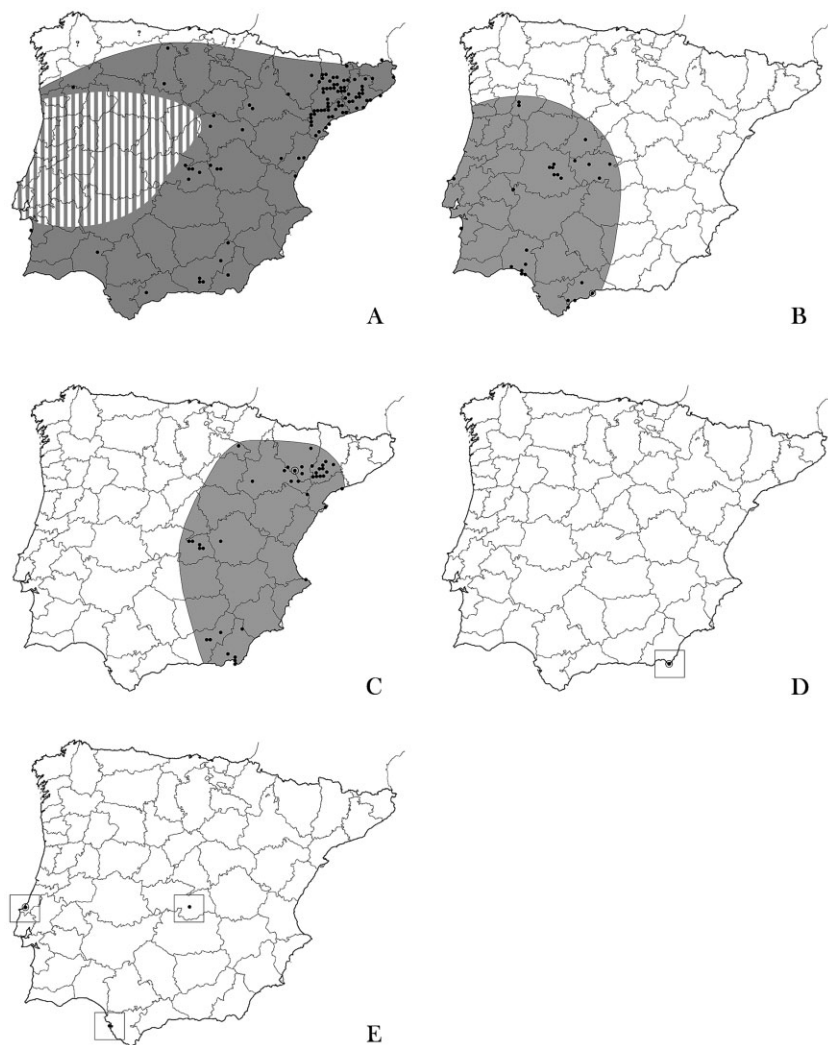


Figure 12. Maps of the known records of: A, *Sphingonotus* (*S.*) *caerulans caerulans*; B, *S. (N.) azurescens*; C, *S. (N.) morini*; D, *S. (N.) almeriense* sp. nov.; E, *S. (N.) nodulosus* sp. nov. Filled circles: material studied by the authors; open circles: records from the literature (only unproblematic species considered); circled records: type localities.

temperate taxa, which lost large parts of their northern geographical range and only survived in southern refugia, the distribution of Mediterranean taxa was also negatively influenced during periods of cool climate. However, the range retractions were probably much smaller and these taxa may have been isolated and survived in several micro-refugia (Çiplak, 2004; Schulte *et al.*, 2012). For the Iberian Peninsula such patterns have been documented, for example, for plants (Olalde *et al.*, 2002; Macaya-Sanz *et al.*, 2012), amphibians (Martínez-Solano *et al.*, 2006), reptiles (Paulo *et al.*, 2001; Carretero, 2008; Santos *et al.*, 2012; Velo-Antón *et al.*, 2012), and mammals (Paupério *et al.*, 2012). Some of these exam-

ples show striking similarities to our results; this is particularly true for other thermophilic taxa. Coastal glacial refugia on the Iberian Peninsula have been postulated for lizards (Carretero, 2008) and snakes (Santos *et al.*, 2012; Velo-Antón *et al.*, 2012), including the area of the Cabo de Gata-Níjar as a refuge for *Podarcis hispanica* (similar to *S. almeriense*), the Gibraltar region for *Podarcis vaucheri* (similar to *S. nodulosus* and *S. imitans*), and the southern Portuguese Atlantic coast for *Podarcis carbonelli* (similar to *S. lusitanicus*) (Carretero, 2008). It might thus be feasible to draw general conclusions on the function of certain coastal regions of the Iberian Peninsula as refugia for xerothermophilic taxa.

ACKNOWLEDGEMENTS

We thank Alexander Benediktov and Bernard Defaut for valuable comments on *Sphingonotus* and fruitful discussions. We are grateful to Judith Marshall and George Beccaloni (NHM), Willem Hogenes (ZMA), Michael Ohl (MfN), Roy Danielsson (MZLU), Daniel Otte, Jason Weintraub (ANSP), and Glória Masó (MCNB) for providing access to museum collections and to Harald Bruckner (Naturhistorisches Museum Wien) for his collaboration in the search of the type material of *Oedipoda callosa*. We also thank the following friends and colleagues, who helped us to collect specimens: Rolf Angersbach, Francisco Barros, Daniel Fernández Ortín, Sónia Ferreira, Yvonne Görzig, Julia Gröning, Jorge Íñiguez Yarza, Gerold Kilzer, Judith Kochmann, Thomas Kordges, Michel Lecoq, Paulo Lemos, Bruno Massa, Tim McNary, M^a.J. Miranda Arabolaza, Carlos Muñoz Alcón, Felix Pahlmann, Juan Quiñones, Martin Schädler, and Andreas Zehm. Part of this project was financed by grants from the Orthopterists' Society and by the Synthesys project to M.H. Furthermore, we thank Valentin Mingo for help with translation of Spanish texts and Miguel Ángel Domingo for his advice concerning the possible location of the type material of *Oedipoda callosa*. Karin Fischer helped during the laboratory work. Finally, we thank four anonymous reviewers for helpful comments on a previous version of the manuscript.

REFERENCES

- Abdel-Dayem MS, Haggag AA, El-Moursy AA, El-Hawagry MA. 2005. A revision of the genus *Sphingonotus* Fieber (Acrididae, Orthoptera) from Egypt. *Journal of the Egyptian German Society of Zoology* **47**: 1–37.
- Aguirre A, Pascual F. 1987. Clave para la identificación de los ortópteros de la provincia de Almería. *Boletín del Instituto Estudios Almerienses* **7**: 119–143.
- Brooks TM, Mittermeier RA, da Fonseca GAB, Gerlach J, Hoffmann M, Lamoreux JF, Mittermeier CG, Pilgrim JD, Rodrigues ASL. 2006. Global biodiversity conservation priorities. *Science* **313**: 58–61.
- Brooks TM, Mittermeier RA, Mittermeier CG, da Fonseca GAB, Rylands AB, Konstant WR, Flick P, Pilgrim J, Oldfield S, Magin G, Hilton-Taylor C. 2002. Habitat loss and extinction in the hotspots of biodiversity. *Conservation Biology* **16**: 909–923.
- Brunner von Wattenwyl K. 1882. *Prodromus der europäischen Orthopteren*. Leipzig: W. Engelmann.
- Carretero MA. 2008. An integrated assessment of a group with complex systematics: the Iberomaghrebian lizard genus *Podarcis* (Squamata, Lacertidae). *Integrative Zoology* **3**: 247–266.
- Carstens BC, Knowles LL. 2007. Estimating species phylogeny from gene-tree probabilities despite incomplete lineage sorting: an example from *Melanoplus* grasshoppers. *Systematic Biology* **56**: 400–411.
- Chopard L. 1943. *Faune de l'Empire Français. I. Orthoptéroïdes de l'Afrique du Nord*. Paris: Larose.
- Çiplak B. 2004. Systematics, phylogeny and biogeography of *Anterastes* (Orthoptera, Tettigoniidae, Tettigoniinae): evolution within a refugium. *Zoologica Scripta* **33**: 19–44.
- Cowling RM, Rundel PW, Lamont BB, Arroyo MK, Arianooutso M. 1996. Plant diversity in Mediterranean-climate regions. *Trends in Ecology & Evolution* **11**: 362–366.
- Coyne JA, Orr HA. 1989. Patterns of speciation in *Drosophila*. *Evolution* **43**: 362–381.
- Defaut B. 2003. Les *Sphingonotus* du groupe *rubescens* en France et en Espagne continentale. *Matériaux Orthoptériques et Entomocénétiques* **8**: 99–127.
- Defaut B. 2005a. Considerations taxonomiques sur *Oedipoda arenaria* Lucas. *Matériaux Orthoptériques et Entomocénétiques* **10**: 25–33.
- Defaut B. 2005b. Note complémentaire sur les *Sphingonotus* du groupe *rubescens* en région paléarctique occidentale (Caelifera, Acrididae, Oedipodinae). *Matériaux Orthoptériques et Entomocénétiques* **10**: 63–72.
- Defaut B. 2005c. *Pseudosphingonotus morini* sp. n. et *P. luciapomaresi* sp. n., deux espèces nouvelles en Espagne (Acrididae, Oedipodinae). *Matériaux Orthoptériques et Entomocénétiques* **10**: 49–55.
- Eades DC, Otte D, Cigliano MM, Braun H. 2013. Orthoptera species file online version 2.0/4.1. <http://orthoptera.speciesfile.org/HomePage/Orthoptera/OrthopteraHomePage.aspx>
- Farris JS, Källersjö M, Kluge AG, Bult C. 1995. Constructing a significance test for incongruence. *Systematic Biology* **44**: 570–572.
- Fieber FX. 1853. Synopsis der europäischen Heuschrecken. *Lotos* **3**: 90–129.
- Funk DJ, Omland KE. 2003. Species-level paraphyly and polyphyly: frequency, causes, and consequences, with insights from animal mitochondrial DNA. *Annual Review of Ecology, Evolution and Systematics* **34**: 397–423.
- García MD, Clemente ME, Hernández A, Presa JJ. 1997. First data on the communicative behaviour of three Mediterranean grasshoppers (Orthoptera: Acrididae). *Journal of Orthoptera Research* **6**: 113–116.
- Gómez A, Lunt DH. 2006. Refugia within refugia: patterns of phylogeographic concordance in the Iberian Peninsula. In: Weiss S, Ferrand N, eds. *Phylogeography in Southern European refugia: evolutionary perspectives on the origins and conservation of European biodiversity*. Amsterdam: Springer, 155–182.
- Harz K. 1975. *Die Heuschrecken Europas, Volume II*. The Hague: Dr. W. Junk N. V.
- Hebert PDN, Penton EH, Burns JM, Janzen DH, Hallwachs W. 2004. Ten species in one: DNA barcoding reveals cryptic species in the neotropical skipper butterfly *Astrartes fulgerator*. *Proceedings of the National Academy of Sciences of the United States of America* **101**: 14812–14817.
- Hewitt G. 2000. The genetic legacy of the Quaternary ice ages. *Nature* **405**: 907–913.

- Hewitt GM. 1999.** Post-glacial re-colonization of European biota. *Biological Journal of the Linnean Society* **68**: 87–112.
- Hochkirch A. 2001.** A phylogenetic analysis of the East African grasshopper genus *Afrophlaeoba* Jago, 1983 (Orthoptera: Acridoidea: Acrididae). PhD dissertation, University of Bremen.
- Hochkirch A, Görzig Y. 2009.** Colonization and speciation on volcanic islands: phylogeography of the flightless grasshopper genus *Arminda* (Orthoptera, Acrididae) on the Canary Islands. *Systematic Entomology* **34**: 188–197.
- Hochkirch A, Husemann M. 2008.** A review of the Canarian Sphingonotini with description of a new species from Fuerteventura (Orthoptera: Acrididae, Oedipodinae). *Zoological Studies* **47**: 495–506.
- Husemann M, Hochkirch A. 2007.** Notizen zur Heuschreckenfauna (Insecta, Orthoptera) von Fuerteventura (Kanarische Inseln, Spanien). *Entomologie heute* **19**: 59–74.
- Husemann M, Namkung S, Habel JC, Danley PD, Hochkirch A. 2012.** Phylogenetic analyses of band-winged grasshoppers (Orthoptera, Acrididae, Oedipodinae) reveal convergence of wing morphology. *Zoologica Scripta* **41**: 515–526.
- Husemann M, Ray J, Hochkirch A. 2011.** A revision of the subgenus *Parasphingonotus* Benediktov & Husemann, 2009 (Orthoptera: Oedipodinae: Sphingonotini). *Zootaxa* **2916**: 51–61.
- Kiefer A, Mayer F, Kosuch J, von Helversen O, Veith A. 2002.** Conflicting molecular phylogenies of European long-eared bats (Plecotus) can be explained by cryptic diversity. *Molecular Phylogenetics and Evolution* **25**: 557–566.
- Kim KC, Byrne LB. 2006.** Biodiversity loss and the taxonomic bottleneck: emerging biodiversity science. *Ecological Research* **21**: 794–810.
- La Greca M. 1994.** Ortoteri italiani nuovi o poco noti. *Memorie della Società Entomologica Italiana* **72**: 211–220.
- Llorente V, Presa JJ. 1997.** *Los Pamphagidae de la Península Ibérica (Insecta: Orthoptera: Caelifera)*. Murcia: Universidad de Murcia.
- Llucià-Pomares D. 2006.** Descripción de *Sphingonotus gypsicola* sp. n. (Caelifera: Acrididae: Oedipodinae) del altiplano central de Cataluña (España). *Boletín Sociedad Entomológica Aragonesa* **39**: 1–25.
- Macaya-Sanz D, Heuert M, López-de-Heredia U, de-Lucas AI, Hidalgo E, Maestro C, Prada A, Alía R, González-Martínez SC. 2012.** The Atlantic-Mediterranean watershed, river basins and glacial history shape the genetic structure of Iberian poplars. *Molecular Ecology* **21**: 3593–3609.
- Maddison WP, Knowles LL. 2006.** Inferring phylogeny despite incomplete lineage sorting. *Systematic Biology* **55**: 21–30.
- Martínez-Solano I, Teixeira J, Buckley D, García-París M. 2006.** Mitochondrial DNA phylogeography of *Lissotriton boscai* (Caudata, Salamandridae): evidence for old, multiple refugia in an Iberian endemic. *Molecular Ecology* **15**: 3375–3388.
- Mason DJ, Butlin RK, Gacesa P. 1995.** An unusual mitochondrial-DNA polymorphism in the *Chorthippus biguttulus* species group (Orthoptera, Acrididae). *Molecular Ecology* **4**: 121–126.
- Medail F, Quezel P. 1999.** Biodiversity hotspots in the Mediterranean basin: setting global conservation priorities. *Conservation Biology* **13**: 1510–1513.
- Mistshenko L. 1936.** Orthoptera Palaearctica critica XII Revision of Palaearctic species of the genus *Sphingonotus* Fieber (Orth. Acrid.). *Eos* **12**: 65–282.
- Moore WS. 1995.** Inferring phylogenies from mtDNA variation – Mitochondrial gene trees versus nuclear gene trees. *Evolution* **49**: 718–726.
- Nylander JAA. 2004.** *MrModeltest*, v2. Uppsala: Evolutionary Biology Centre, Uppsala University.
- Olalde M, Herran A, Espinel S, Goicoechea PG. 2002.** White oaks phylogeography in the Iberian Peninsula. *Forest Ecology and Management* **156**: 89–102.
- Pardo JE, Gómez R, Del Cerro A. 1991.** Claves de determinación de los Orthopteroidea de los principales sistemas montañosos de Castilla-La Mancha. *Al-Basit* **29**: 119–193.
- Paulo OS, Dias C, Bruford MW, Jordan WC, Nichols RA. 2001.** The persistence of Pliocene populations through the Pleistocene climatic cycles: evidence from the phylogeography of an Iberian lizard. *Proceedings of the Royal Society B-Biological Sciences* **268**: 1625–1630.
- Paupério J, Herman JS, Melo-Ferreira J, Jaarola M, Alves PC, Searle JB. 2012.** Cryptic speciation in the field vole: a multilocus approach confirms three highly divergent lineages in Eurasia. *Molecular Ecology* **21**: 6015–6032.
- Rambaut A, Drummond AJ. 2009.** Tracer v1.5. <http://tree.bio.ed.ac.uk/software/tracer/>
- Rivas-Martínez S. 1987.** *Memoria del mapa de series de vegetación de España. 1:400.000*. Madrid: Ministerio de Agricultura PyA.
- Ronquist F, Huelsenbeck JP. 2003.** MrBayes 3: Bayesian phylogenetic inference under mixed models. *Bioinformatics* **19**: 1572–1574.
- Santos X, Rato C, Carranza S, Carretero MA, Pleguezuelos JM. 2012.** Complex phylogeography in the Southern Smooth Snake (*Coronella girondica*) supported by mtDNA sequences. *Journal of Zoological Systematics and Evolutionary Research* **50**: 210–219.
- Schulte U, Hochkirch A, Lotters S, Rodder D, Schweiger S, Weimann T, Veith M. 2012.** Cryptic niche conservatism among evolutionary lineages of an invasive lizard. *Global Ecology and Biogeography* **21**: 198–211.
- Shaw KL. 2002.** Conflict between nuclear and mitochondrial DNA phylogenies of a recent species radiation: what mtDNA reveals and conceals about modes of speciation in Hawaiian crickets. *Proceedings of the National Academy of Sciences of the United States of America* **99**: 16122–16127.
- Smith MA, Woodley NE, Janzen DH, Hallwachs W, Hebert PDN. 2006.** DNA barcodes reveal cryptic host-specificity within the presumed polyphagous members of a genus of parasitoid flies (Diptera: Tachinidae). *Proceedings of the National Academy of Sciences of the United States of America* **103**: 3657–3662.

- Swofford DL. 2002.** *PAUP**. *Phylogenetic analysis using parsimony (*and other methods)*. Version 4. Sunderland, MA: Sinauer Associates.
- Toews DPL, Brelsford A. 2012.** The biogeography of mitochondrial and nuclear discordance in animals. *Molecular Ecology* **21**: 3907–3930.
- Uvarov B. 1948.** Andalusian Orthoptera described by Rambur. *Eos* **24**: 369–390.
- Velo-Antón G, Godinho R, Harris DJ, Santos X, Martínez-Freiria F, Fahd S, Larbes S, Pleguezuelos JM, Brito JC. 2012.** Deep evolutionary lineages in a Western Mediterranean snake (*Vipera latastei/monticola* group) and high genetic structuring in Southern Iberian populations. *Molecular Phylogenetics and Evolution* **65**: 965–973.
- Vieites DR, Wollenberg KC, Andreone F, Kohler J, Glaw F, Vences M. 2009.** Vast underestimation of Madagascar's biodiversity evidenced by an integrative amphibian inventory. *Proceedings of the National Academy of Sciences of the United States of America* **106**: 8267–8272.
- Wilcox TP, Hugg L, Zeh JA, Zeh DW. 1997.** Mitochondrial DNA sequencing reveals extreme genetic differentiation in a cryptic species complex of neotropical pseudoscorpions. *Molecular Phylogenetics and Evolution* **7**: 208–216.
- Willemse F, Willemse L. 2008.** An annotated checklist of the Orthoptera–Saltatoria from Greece including an update bibliography. *Articulata Beiheft* **13**: 1–91.

SUPPORTING INFORMATION

Additional Supporting Information may be found in the online version of this article at the publisher's web-site:

Table S1. Overview of samples used for molecular analyses.